Development of new dendrochronology in tropics using oxygen isotope ratios and its application to a 400-year hydroclimate reconstruction in northern Southeast Asia

(酸素同位体比を用いた熱帯における新しい年輪年代法の開発とその東南アジア北部における過去 **400** 年間の水循環復元への応用**)**

Chenxi Xu

（許 晨曦）

A dissertation for the degree of Doctor of Science
Department of Earth and Environmental Sciences,
Graduate School of Environmental Studies, Nagoya University

（名古屋大学大学院環境学研究科地球環境科学専攻学位論文 博士 （理学））

2013

Abstract

Monsoon and El Nino southern Oscillation (ENSO) variations, especially associated precipitation changes, have an important effect on agrarian economy of densely populated regions in Southeast Asia and civilizations shift during the past several hundreds of years. However, the instrumental meteorological records in Southeast Asia are temporally and spatially limited. Therefore, long-term tree ring records are necessary for improving our understanding of Asian summer monsoon and ENSO variability.

However, there are two difficulties to hinder the development of tree ring research in tropical area. One is that ring boundaries of tropical tree are often not distinct, so it is hard to get the basic information (annual growth) for forest and tree ring research. The other is that the correlations between the tree ring width time series of different trees are very low because of ecological disturbance, which result in difficulty in cross-dating using ring width and climate reconstruction based on relationships between ring width-climate parameters.

Therefore, a new proxy which can be used for measuring annual growth for trees without clear ring boundary and can be climate-sensitive is needed. Tree ring cellulose $\delta^{18}O$ seems to be such a good proxy to solve the problems in tree ring research in tropical area based on tree ring cellulose $\delta^{18}O$ fractionation model.

At first, I analyzed intra-annual variations of tree ring cellulose $\delta^{18}O$ for trees without distinct rings (*Styrax* and *Ficus sp*) in northern Laos, and found that there were clear annual cycles of tree ring cellulose $\delta^{18}O$ of *Styrax* and *Ficus sp*, which can be used for measuring annual growth for tropical trees without distinct annual rings.

I measured tree ring cellulose $\delta^{18}O$ of seven cores (*Fokienia hodginsii* with

clear ring boundary) with annual-resolution in natural forest in northern Laos during the period of 1588-2002, and found that compared with tree ring width, tree ring cellulose $\delta^{18}O$ shows more consistent variations between different trees, displays higher signal strengths and has significant correlations with climatic parameters (precipitation, Palmer Drought Severity Index (PDSI) and temperature), which indicate that tree ring cellulose $\delta^{18}O$ can provide a useful method to cross-date tree samples, especially for trees in tropical areas that cannot be cross-dated using ring width due to frequent endogenous disturbance or the lack of distinct limiting factors for tree growth.

After solving the cross-dating problem, I reconstructed the monsoon season PDSI based on the linear regression between PDSI and tree ring cellulose $\delta^{18}O$. Reconstructed PDSI shows that the wetter periods were identified as AD 1660-1695, AD 1705-1790, whereas the drier periods mainly occurred during AD 1630–1660, AD 1900-1940 and AD 1954-2002, and a decreasing trend of moisture in monsoon season over the last 200 years. Reduction of Asian summer monsoon intensity can be also found across other tree ring cellulose $\delta^{18}O$ records from the Himalaya, Tibet Plateau and Southeast Asia. Increasing sea surface temperatures (SST) in tropical Indian Ocean and Pacific may weaken Asian summer monsoon intensity.

The correlation analysis between tree ring cellulose $\delta^{18}O$ and global SST /the Multivariate El Niño-Southern Oscillation (ENSO) Index (MEI) during period of 1872-2002 indicate that ENSO has significant influences on tree ring cellulose $\delta^{18}O$ in northern Laos. Combining ENSO-sensitive proxy (tree ring cellulose $\delta^{18}O$ of *Fokienia hodginsii*) in Laos and Vietnam, annual MEI and local ENSO events history are reconstructed during the period of 1605-2002, which is consistent with global ENSO events.

Contents

List of Tables

List of Figures

Figures (cont.) Page

1. Introduction

Paleoclimatology is the study on earth's climate before the period with instrumental meteorological data. Instrumental records just cover a small fraction of the climate of earth, and so climatic variation and the evolution of climate is not clear. Long-term climate information can be got based on the climate-dependent physical, chemical and biological processes. Since a detailed and reliable record of past climatic variation is built up, the possibility that identify causes and mechanisms of climate change is increased. Thus, paleoclimatic data provide the basis for evaluating hypotheses on the causes of climatic change. Only when the causes of past climatic variations are understood will it be possible to fully anticipate or forecast climatic variations in the future.

Asian summer monsoon that impacts on very large area in Asia is a very complex component of the global climate system (Figure 1.1). Droughts and extreme flooding have affected people who live in monsoonal Asia during the past millennium (Figure 1.2). Some studies (Buckley et al., 2010; Cook et al., 2010; Yancheva et al., 2007; Zhang et al., 2008) show that variations of Asian monsoon have an important effect on culture collapse and society development.

Although Asian summer monsoon has great influences on human populations and ecosystems, the knowledge on long-term variability of the Asian summer monsoon is not enough. In fact, climate models cannot simulate the Asian summer monsoon (Kripalani et al., 2007) and related tropical Indo-Pacific forcing (Vecchi et al., 2008) accurately Therefore, the issues, such as the mechanisms which control the Asian summer monsoon, and how Asian

summer monsoon will change under the background of global warming, are still not clear.

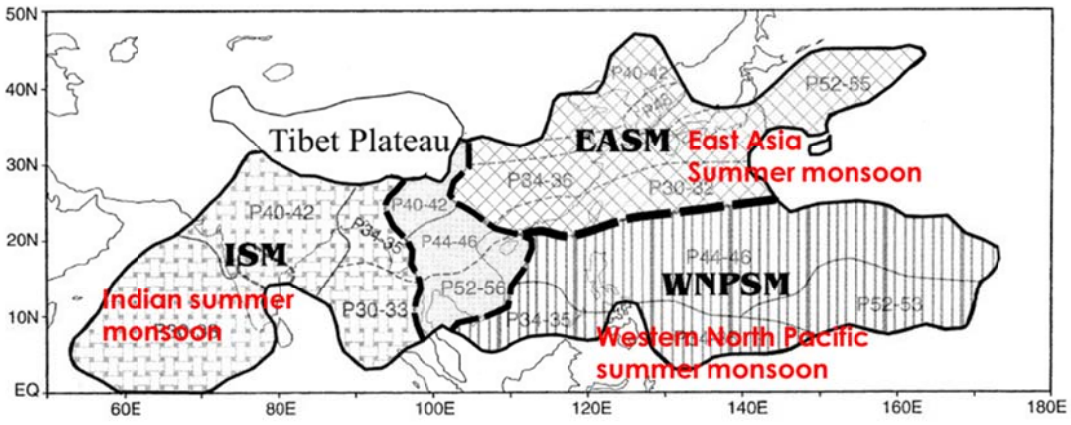

Figure 1.1 Three subregions (Indian summer monsoon, East Asia summer monsoon and Western North Pacific summer monsoon) of the Asian–Pacific monsoon. (Modified from Wang and Holin., 2001)

High-resolution paleoclimatic records are highly needed. However, there are a lot of high-resolution proxy observations used for paleoclimate and paleoenvironmental studies in the globe except in the Asian subtropics controlled by Asian monsoon (Figure 1.3). Corals (Abram et al., 2008), ice cores (Thompson et al., 2006), lake sediments (Yancheva et al., 2007), speleothems (Zhang et al., 2008) has been used for reconstructing the history of Asian Monsoon. However, by their nature, these records are restricted for special location due to their spatial and/or temporal resolution. Besides, some of them cannot correlate with modern meteorological data by annual resolution.

Figure 1.2 Flood and drought in South East Asia

a, Flood at Thailand, 2007; b, Drought near Vientiane which is capital of Laos, March, 2010 (http://www.rfa.org/english/)

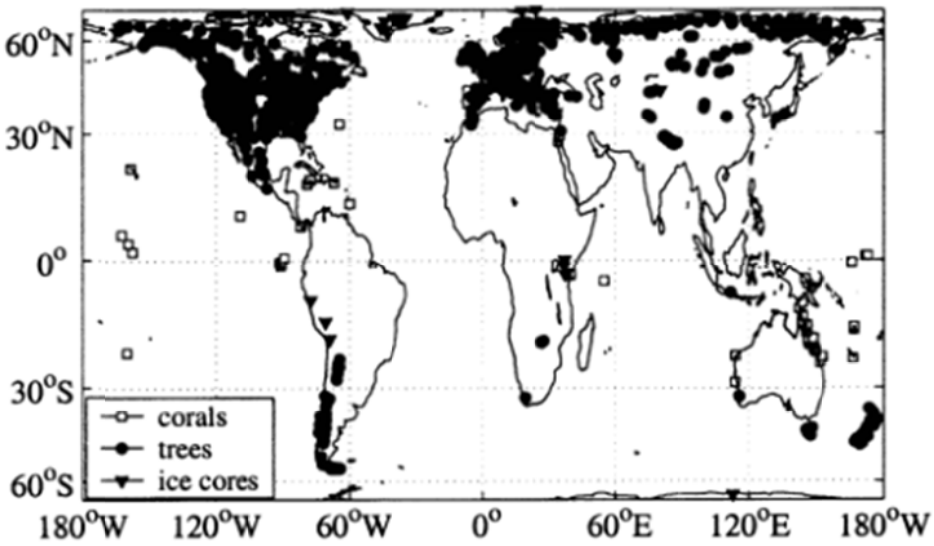

Figure 1.3 Sites of high-resolution coral, tree-ring and ice core records in the Paleoclimatology electronic database (http://www.ngdc.noaa.gov/paleo/) (Modified from Evans et al., 2004).

Tree rings are obvious candidates for paleoclimate reconstruction due to its high-resolution and accurate chronology and widespread, then it is possible to test spatial changes of paleoclimate (Fritts, 1976).

Although trees are widespread in tropic areas, until recently, there have been very few tree-ring studies by traditional methods in tropical regions (Figure 1.3) (Rozendaal and Zuidema, 2011). The seasonality in rainfall, relative humidity and temperature in the tropics is not large enough, so annual tree rings are often irregular, indistinct, even not present at all. However, in monsoon-influenced tropical areas, because there is a distinct dry season, dendroclimate research is possible. In Southeast Asia, several tree ring studies have been carried out during the recent two decades to find suitable tree species for dendroclimatology and to get more information on the Asian summer monsoon in the past (Buckley et al. 1995, 2005, 2007a, 2010; D'Arrigo et al. 1997; Sano et al., 2009).

Although computer programs such as COFECHA (Holmes, 1983) can provide reliable statistics tests on cross-dating, the correlations between ring width and climate parameter are still relative low (Buckley et al., 2007a), which are cannot be used for paleoclimate reconstruction. Despite the recent progress in paleoclimatic reconstruction by ring width in Southeast Asia (Sano et al., 2009; Buckley et al., 2010), the monsoon season signal is not available, because ring widths in this region mainly reflect the influence of early monsoon (March-April-May) climates, and hence do not provide a record of actual summer monsoon variability. In addition, the ring width chronology is affected by non-climatic disturbances (especially those related to closed-canopy environmental conditions).

Tree-ring cellulose $\delta^{18}O$ exhibits certain advantages on paleoclimate reconstruction over the approach using tree-ring widths in some cases. First, the physiological controls of tree-ring cellulose $\delta^{18}O$ are well understood (Flanagan et al., 1991; Roden et al., 2000; Sternberg et al., 1986; Yakir and DeNiro, 1990). Second, tree-ring cellulose $\delta^{18}O$ is not as strongly affected by

the physiological characteristics of individual trees as ring width is (Raffalli-Delerce et al., 2004), and it has a limited effect of age and a lower autocorrelation (McCarroll and Loader, 2004; Shi et al., 2011). Third, tree-ring cellulose $\delta^{18}O$ can be employed as a chronometer and climatic indicator for trees lacking visible rings (Anchukaitis et al., 2008; Anchukaitis and Evans, 2010; Evans and Schrag, 2004; Poussart and Schrag, 2005; Poussart et al., 2004) and can supply an intra-annual resolution signal (Managave et al., 2010; Roden et al., 2009). Fourth, for trees not growing at their "ecological" limit, it is possible to extract a strong climate signal using stable isotope methods, where ring widths (and density) do not routinely yield useful climatic information (Loader et al., 2008).

In addition, previous isotope dendrochronology research (Nakatsuka, 2004) indicated that variations in tree-ring width and its carbon isotopic composition ($\delta^{13}C$) often show large discrepancies between different individual trees in humid and temperate regions. However, even in these cases the tree-ring $\delta^{18}O$ of different trees are well correlated with each other, and the common signal reflect the regional climate changes.

Therefore, I analyzed intra-annual and inter-annual tree ring cellulose $\delta^{18}O$ variations of *Fokienia* in Laos and Vietnam, reconstructed monsoon season local hydroclimate changes and evaluated local influences of ENSO during the last 400 years.

2 Oxygen isotope theory in tree-ring

Libby et al. (1976) found that tree-rings oxygen isotope ratios in two German oak trees (*Quercus petraea*) were correlated with temperature. Then oxygen isotopes in tree rings are seen as a powerful tool for the reconstruction of past atmospheric conditions such as the isotopic composition of precipitation, air temperature (Burk & Stuiver, 1981) based on the empirical relationships. However, the physiological mechanism of oxygen isotope in tree-ring cellulose had not been fully understood, and these apparent empirical relationships are not robust all the times within different climate zone and tree species.

Therefore, the knowledge on the physiological and biochemical processes, which control tree ring oxygen isotope during the process of cellulose formation, is needed.

For origination of oxygen isotope signal, as we know, both carbon dioxide (CO_2) and water (H_2O) provide oxygen atoms (O) to carbohydrate during the metabolism, which has significant contribution to oxygen isotope signal in cellulose. DeNiro and Epstein (1979) measured the oxygen-18/oxygen-16 ratios ($^{18}O/^{16}O$) of cellulose, which was derived from two sets of wheat plants grown under same conditions in all respects, the only difference between two groups of wheat plant is the oxygen isotope ratios of carbon dioxide. They found that the difference in the oxygen isotope ratios of the cellulose between two groups of wheat plant is almost same with the difference in the oxygen isotope ratios of water in wheat plants. These results revealed that the oxygen atom from water in the plant exchanged completely with oxygen atom from carbon dioxide in the process of cellulose formation.

Because there is no isotopic fractionation during the transportation of water from soil to leaf (White et al., 1985) and because the isotopic signature of xylem water is imprinted on the final cellulose product (Deniro and Epstein,

1979), many models of tree-ring cellulose $\delta^{18}O$ focus on two processes: (1) changes in the oxygen isotope ratio of water as it moves through the plant (effect of leaf water enrichment) and (2) changes in the isotope ratio of oxygen as it becomes incorporated in the cellulose molecule through biochemical effects (Sternberg, 2009).

The isotopic composition of leaf water is modified from xylem water by transpiration, which leads to a consequent enrichment of the $\delta^{18}O$ of the leaf water. This process, described by Craig and Gordon (1965),

$$\delta^{18}O_l = \delta^{18}O_x + \varepsilon^* + \varepsilon_k + e_a / e_i\left(\delta^{18}O_a - \varepsilon_k - \delta^{18}O_x\right) \quad (1)$$

Where the subscripts l, x and a refer to leaf water, xylem water and water vapor in the air outside the leaf, respectively. ε^* and ε_k are the equilibrium and kinetic isotopic fractionation factors, respectively. During the process of photosynthesis, sucrose is produced in the leaves by combining water and CO_2. Sucrose is then transported to the trunk where a portion of oxygen atoms from sucrose undergo isotopic exchange with xylem water during the process of formation of cellulose. During these processes, we assumed that the xylem water is at equilibrium with atmospheric water vapor, and that the ambient temperature is similar with leaf temperature, $\delta^{18}O_a$ can be equal to $\delta^{18}O_p - \varepsilon^*$, and e_a/e_i is the ambient water vapor pressure/intercellular water vapor pressure ratio, which was considered as the relative humidity (h) (Dongmann et al.,1974). The Craig-Gordon model for evaporation can be simplified as:

$$\delta^{18}O_l = \delta^{18}O_p + (\varepsilon^* + \varepsilon_k)(1-h) \quad (2)$$

Eq. (2) demonstrates that oxygen isotope of leaf water is mainly controlled by relative humidity and oxygen isotope of source water.

However, some studies have found that the oxygen isotope of leaf water derived from Craig-Gordon model is higher than observed oxygen isotope of in

bulk leaf water measurements (Allison et al., 1985; Flanagan et al., 1991). These differences are derived from the fact that enriched water from the evaporating sites mixed with depleted xylem water. This phenomenon is called the Péclet effect (Barbour et al., 2000). Barbour et al. (2004) modified the Craig–Gordon model to contain the potential influence, which was brought in by the Péclet effect. The bulk leaf oxygen isotope is simulated by the following equation (Sternberg, 2009):

$$\delta^{18}\mathrm{O}_{\mathrm{L}} = (1-\alpha)\delta^{18}\mathrm{O}_{\mathrm{s}} + \alpha\delta^{18}\mathrm{O}_{l} \tag{3}$$

Where $\delta^{18}O_L$ represents the $\delta^{18}O$ of bulk leaf water, α is the fraction of enriched water. Sternberg (2009) provided the controlling factors of stem cellulose oxygen isotope during the processes from the leaf water to the stem cellulose, as expressed in Eq. (4):

$$\delta^{18}\mathrm{O}_{\mathrm{c}} = \mathrm{f}_0\left(\delta^{18}\mathrm{O}_{\mathrm{p}} + \varepsilon_o\right) + (1-\mathrm{f}_0)\left(\delta^{18}\mathrm{O}_{\mathrm{L}} + 27‰\right) \tag{4}$$

Eq. (2) and (3) are inserted into Eq. (4), we get:

$$\delta^{18}\mathrm{O}_{\mathrm{c}} = \left(\delta^{18}\mathrm{O}_{\mathrm{s}} + \varepsilon_o\right) + \alpha(1-\mathrm{f}_0)(1-h)\left(\varepsilon^{*} + \varepsilon_k\right) \tag{5}$$

where $\delta^{18}O_c$ represents the $\delta^{18}O$ of tree-ring cellulose, f_o is the exchanged proportion of carbohydrate oxygen with xylem water, ε_o is the net biological isotopic fractionation factor between the xylem water and the exchanged oxygen in the carbohydrate, and +27‰ is the equilibrated isotopic exchange ratio between the leaf water and the photosynthesized carbohydrate (Deniro and Epstein, 1979; Yakir and DeNiro, 1990).

From the Eq. (5), main factors that control tree ring cellulose $\delta^{18}O$ are precipitation oxygen isotope and relative humidity, both of which usually

correlated with precipitation and temperature. Due to different climate condition in different sites, the main controlling factor of tree ring cellulose $\delta^{18}O$ may vary. For example, Evans (2007) indicated tree ring cellulose $\delta^{18}O$ in Costa Rica were controlled by precipitation rather than temperature and relative humidity. Kahman et al. (2011) showed that tree ring cellulose $\delta^{18}O$ in Hawaii is an index of leaf-to-air vapor pressure difference rather than precipitation. Therefore, for paleoclimatic implication of tree ring cellulose $\delta^{18}O$, we still need to analyze correlation between tree ring cellulose $\delta^{18}O$ and climatic parameter case by case.

3 Materials and Methods

3.1 Sampling site

For tree ring annual oxygen isotope analysis, The tree-ring samples used in this study were derived from 5-mm-increment cores collected from old growth *Fokienia hodginsii* (>300 years). These trees grow in the Phu Leuy (PL) mountain area (20°17′N, 103°55′E, 1340 m) in northern Laos (Figure 3.1). Three cores from different directions per tree at breast height were collected in the fall of 2003. Approximately 100 cores were collected. According to the 1961-1990 meteorological data (Figure 3.2) from the Luang Prabang weather station (19.9°N, 101.2°E), which is located 140 km west of Phu Leuy at an elevation of 305 m, the annual mean temperature is 24.4 °C and the mean annual precipitation is 1442.9 mm, 85% of which falls in the monsoon months from May to October.

To test if the tree ring cellulose oxygen isotope can measure the annual growth for trees without distinct annual rings, we collected two 12 mm increment cores of *Ficus sp* and one core of *Shorea sp* at breast height in natural forests and one disk of Styrax (Figure 3.3) from plantation, near Kachet village (Figure 3.1b), Luang Prabang, Laos (20.5°N, 102.3°N, 800 m) in August, 2011. It's about 1km from the natural forests to the plantation.

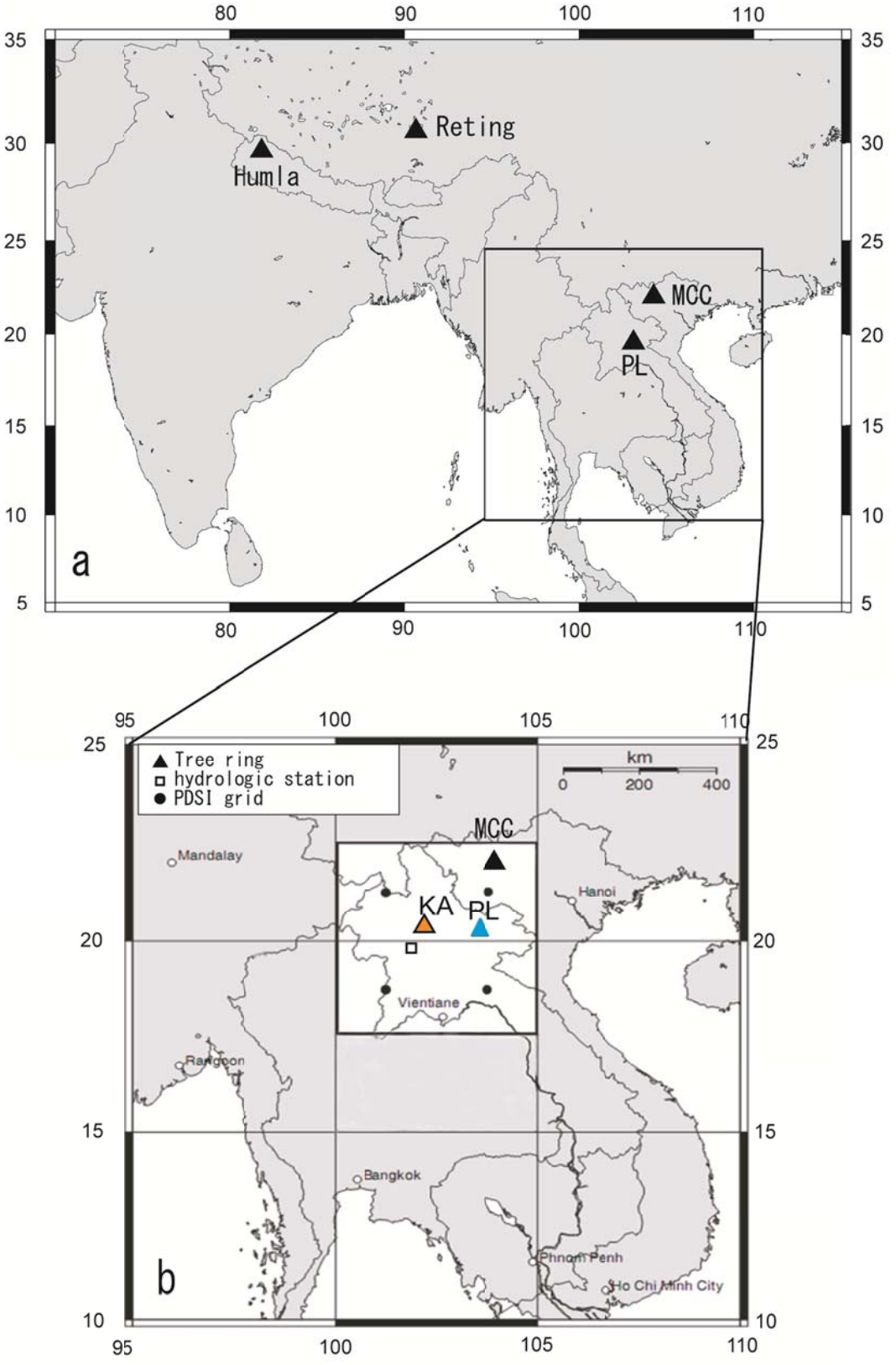
80
90
100
110
35
30
25
20
15
10
5
Reting
Humla
MCC
PL
a
95
100
105
110
25
20
15
10
Tree ring
hydrologic station
PDSI grid
km
0
200
400
MCC
KA
PL
Mandalay
Hanoi
Vientiane
Rangoon
Bangkok
Phnom Penh
Ho Chi Minh City
b

Figure 3.1 a: The study region showing the sampling site Phu Leuy (PL) mountain area (19.9°N, 101.2°E) and tree ring sites in Vietnam (MCC, Sano et al., 2012), in Tibet (Reting, Grießinger et al., 2011) and Himalaya (Humla, Sano et al., 2011), b: the Luang Prabang meteorological and hydrological station, the area of the grid box averages of the CRU TS3.1 and PDSI data sets used in this study is enclosed by the thick solid line, c: monthly mean temperature (black circles) and precipitation (gray bar) (1961–1990) at the Luang Prabang instrumental station.

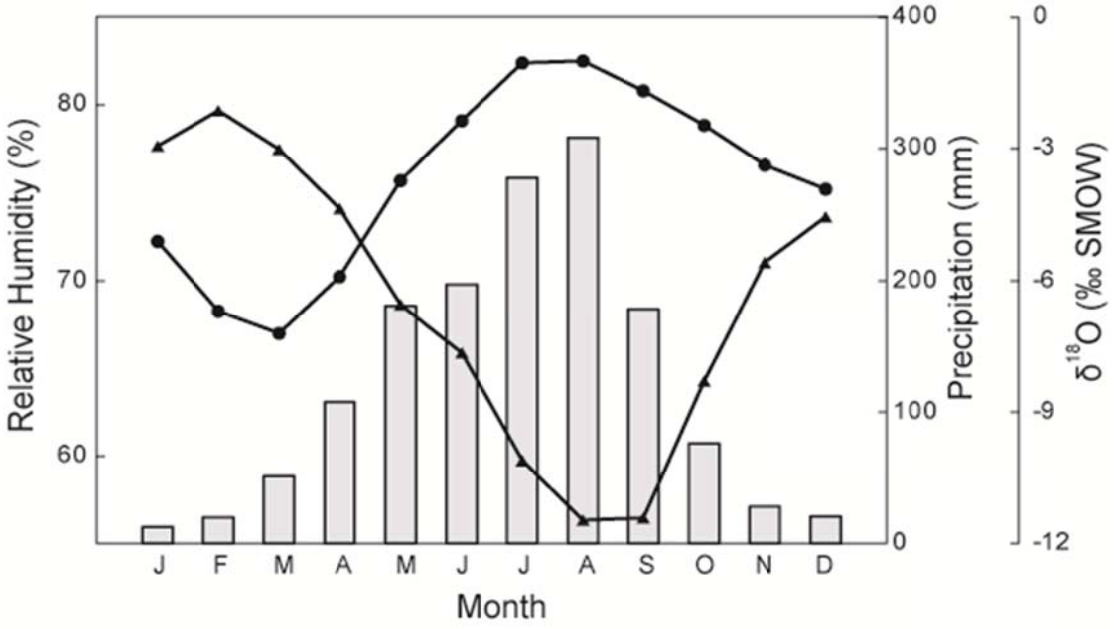

Figure 3.2 Monthly mean relative humidity (spot) and precipitation (bar) at the Luang Prabang meteorological observatory station (1961-1990), monthly modeled precipitation oxygen isotope (triangle) in central Laos (1980-2010) from Yoshimura et al., (2008).

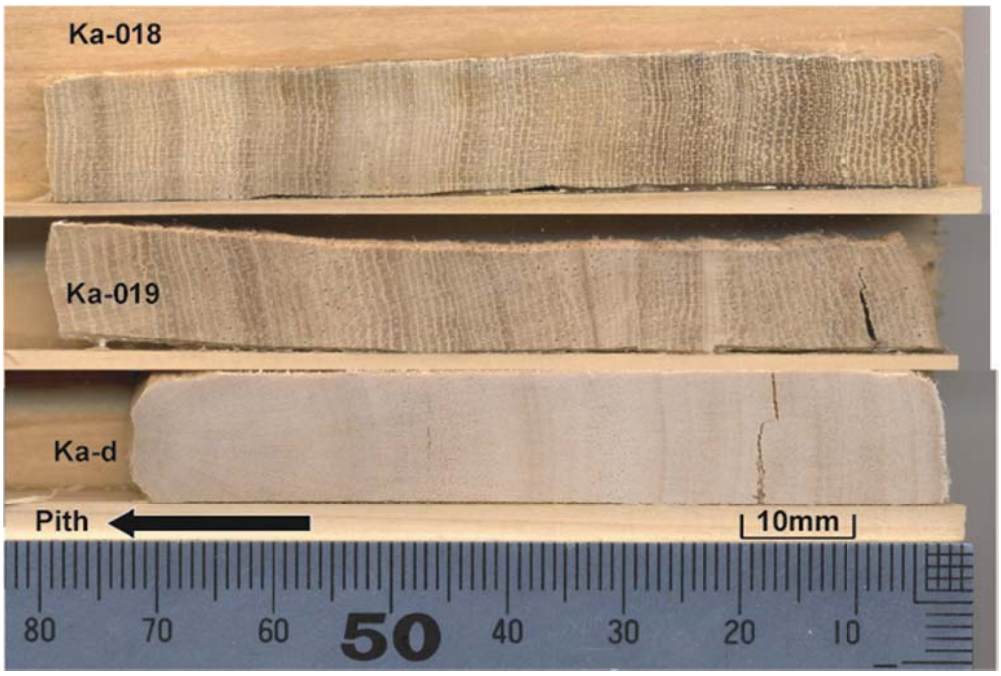

Figure 3.3 Sample photos for *Ficus sp* (Ka-018 and Ka-019) and *Styrax* (Ka-d) for intra-annual tree ring cellulose isotope analysis.

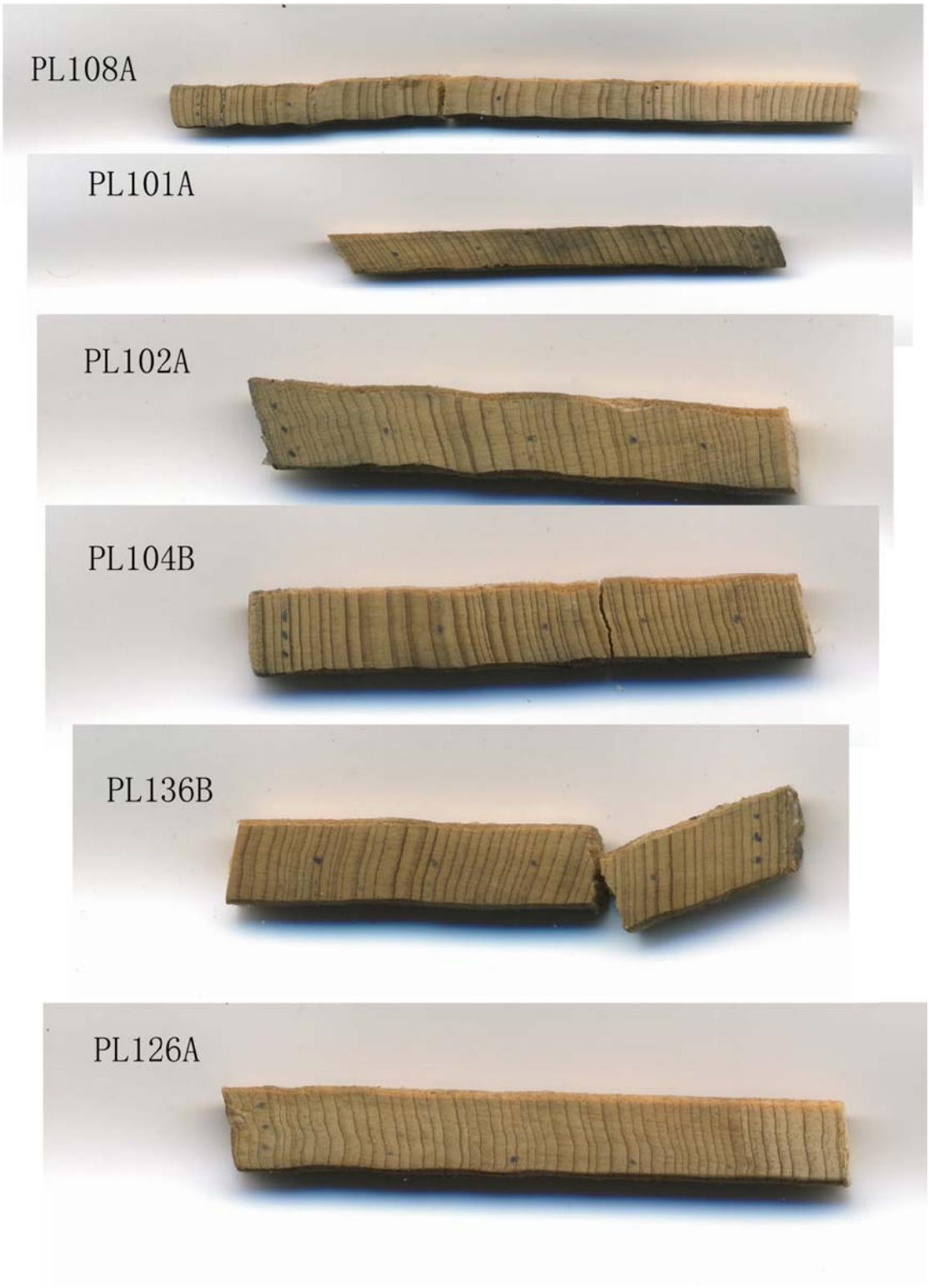

Figure 3.4 Sample photos for *Fokienia hodginsii* for inter-annual tree ring cellulose isotope analysis (PL101A, PL102A, PL104B, PL108A, PL126A and PL136B).

3.2 Cellulose extraction

Cellulose, lignin, waxes, lipids, oils, and resins are the main part of tree rings. The proportion of non-cellulose compounds (lignin, waxes, lipids, oils, and resins) can change significantly throughout tree ring samples (Wilson and Grinsted, 1977; Brendel et al., 2000). Many studies, in which employ tree ring isotope records to find potential paleoclimate information, extract pure cellulose (α-cellulose) (Gaudinski et al., 2005). Oxygen isotope in α-cellulose is considered as a suitable proxy for paleoclimate researches, because after α-cellulose formed, oxygen atoms in tree ring cellulose do not exchange with oxygen atoms in other compounds. So the isotope values at the time of cellulose formation that is helpful to record the environmental information can be preserved in cellulose (Sternberg et al., 1986). For the sample in PL site, the width of many rings is very narrow (~3mm) and most rings did not have distinct earlywood-latewood boundary. Therefore I used whole annual rings, which include earlywood and latewood for the isotopic analyses.

Most researchers separate annual rings before α-cellulose extraction. Each ring was treated independently, so the number of samples per batch was limited. The number of samples per batch of the Brendel (Brendel et al., 2000) and modified Brendel (Evans and Schrag, 2004) methods is 56 and 80, respectively. Given that chemically treating hundreds or thousands of samples is time-consuming, researchers have analyzed wood blocks of 5 or 10 years together for a tree-ring sample with a one-thousand-year length, in which inter-annual variations cannot be retained (Esper et al., 2010; Gagen et al., 2011b). Therefore, a method that can treat hundreds or thousands of rings simultaneously is necessary to save time. I employed “the plate method”, which is similar to Li’s method (Li et al., 2011c). In this method, the α-cellulose is extracted directly from the wood plate rather than individual rings, and the

grinding step is omitted. This method drastically reduces the time needed.

The following is the detailed procedure. Before α-cellulose extraction, I cut cores into plates along surfaces perpendicular to the cellulose fiber directions with a thickness of 1 mm using a low-speed diamond wheel saw (Figure 3.5a and b).

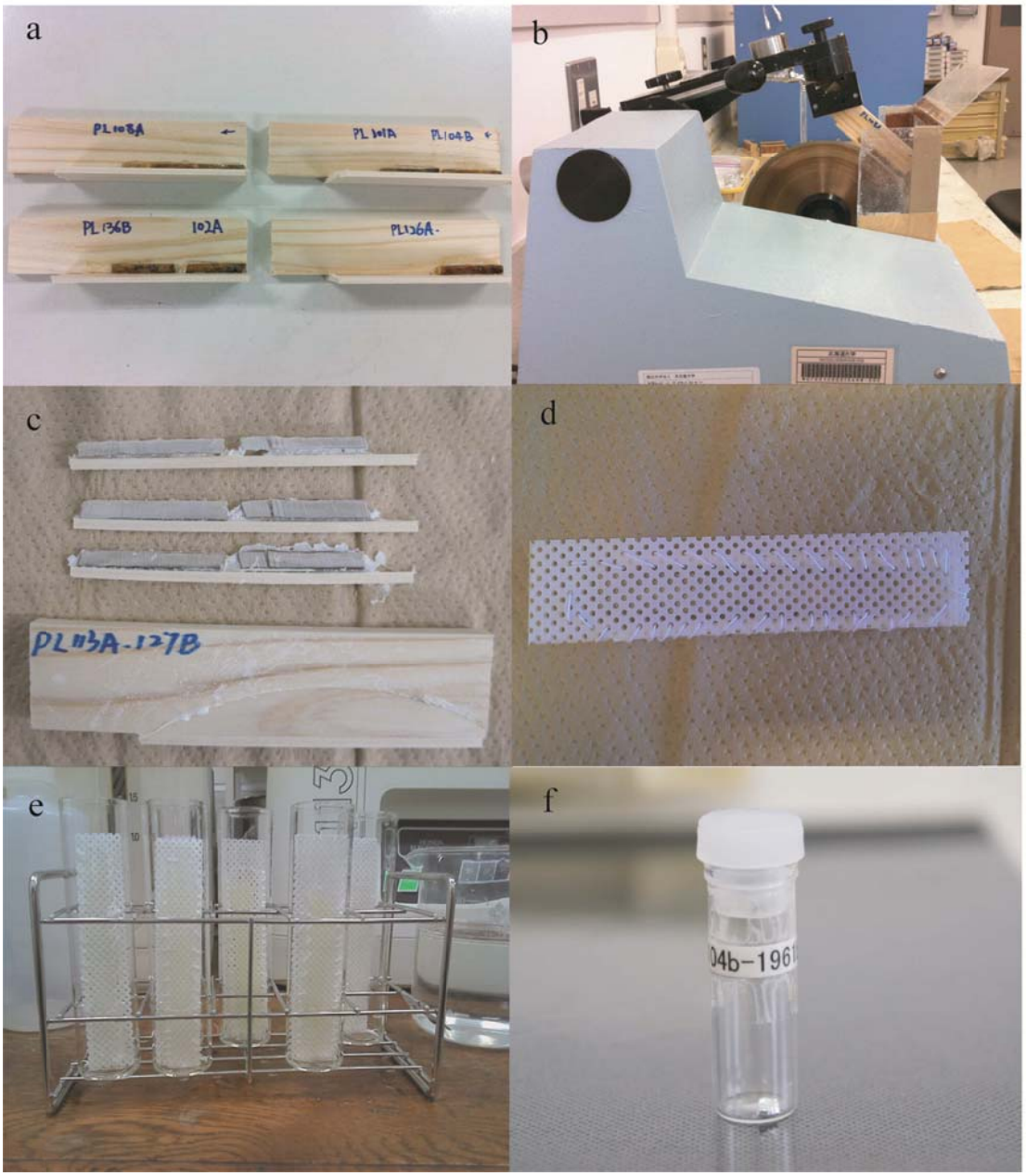

Figure 3.5 a: mounted core samples onto the wood plates, b: cut core sample to plate with the thickness of 1 mm by a low-speed diamond wheel saw, c: plate sample with the thickness of 1 mm, d: bind plate sample with two Teflon

punch sheets, e: cellulose extraction, f: wrap sample with sliver foil.

I then selected one plate with greatest width. In general, one core taken by a 5 mm-increment borer can be cut into two or three plates (1 mm per plate) (Figure 3.5c), while Li et al. (2011c) employed a thickness of 3.5-4.0 mm per plate, which requires more time for the chemical reaction and consumes more samples. Although it depends on the ring widths, one plate is usually enough to produce two samples for isotopic measurement per year. Thus, I can keep another plate to observe and check the wood's anatomy after obtaining isotopic data. To maintain the shape of the wood plate during the α-cellulose extraction, the plate was packed by two Teflon punch sheets and was put into a glass tube for chemical reactions (Figure 3.5d).

The chemical protocol for extracting α-cellulose (Figure 3.5e) from the tree rings generally follows the Jayme and Wise method (Green, 1963; Loader et al., 1997). The glass tube containing the wood plate was treated first with toluene/ethanol (1:1) in an ultrasonic water bath for 30 minutes, then with acetone in an ultrasonic water bath for 30 minutes in a fume hood to remove lipids, and then with an acidified $NaClO_2$ solution in a water bath (70°C) for 60 minutes. The step of decomposing the lignin by acidified $NaClO_2$ solution had to be repeated a few times until the color of the plate turned white. A 17%(wt) NaOH solution was poured into a glass tube containing the wood plate in a water bath (80°C) for 60 minutes to remove hemicellulose, and this step was repeated another two times. After this step, the wood plate was extremely fragile. The wood plate was gently washed with a diluted HCl solution and distilled water.

Figure 3.6 Cellulose plate after chemical treatment and drying process.

The cellulose plate was then dried in an oven overnight. The color of final cellulose plate is white (Figure 3.6). For one batch of samples, the above steps took 4 days. For the purpose of saving time, I extracted many cores simultaneously. The separation of the tree-ring sample from the α-cellulose plate was performed under a binocular microscope.

For the annual tree ring cellulose oxygen isotope of *Fokienia* in PL site (Figure 3.1, blue triangle), I selected 7 trees for isotopic analysis based on the following criteria: 1) the ring widths were wide enough to produce adequate samples for isotopic measurement, and 2) the cores consisted of more than 300 rings (to reduce any potential bias related to age).

For the intra-annul high-resolution tree ring cellulose oxygen isotopes of *Ficus sp* and *Styrax* in KA site (Figure 3.1, orange triangle), I measured *Styrax* by 1 mm resolution. To test whether the apparent rings of *Ficus* (Figure 3.3) are annual rings or not, I analyzed tree ring oxygen isotopes of two cores by apparent rings. I assume that tree ring oxygen isotope of two trees should be highly correlated if the apparent rings of *Ficus* are annual rings, which based on previous tree ring oxygen isotopes of *Fokienia hodginsii* with clear ring structure in Laos (Xu et al., 2011) and Vietnam (Sano et al., 2012).

3.3 Stable isotopic analysis

I loaded duplicate cellulose samples (sample size: 120–180 μg) into silver foil (Figure 3.5f), and determined $^{18}O/^{16}O$ ratios using two isotope ratio mass spectrometers (Delta plus XL and Delta V ADVANTAGE) interfaced with pyrolysis-type elemental analyzers (TC/EA) at the Research Institute of Humanity and Nature, Kyoto, Japan and the Graduate School of Environmental Studies, Nagoya University, Nagoya, Japan. The $^{18}O/^{16}O$ ratios were expressed as $\delta^{18}O$ (‰) deviation relative to V-SMOW standard. The cellulose $\delta^{18}O$ values were calculated by comparison with the laboratory working standards IAEA C3 cellulose and Merck cellulose, which were inserted frequently during the measurement. The oxygen isotope ratios were obtained from the average of the duplicate analyses of the cellulose samples from each annual tree-ring. The analytical uncertainties associated with repeated measurements of the IAEA C3 cellulose and Merck cellulose were 0.18‰ (n = 108) and 0.12‰ (n = 361) (1σ), respectively.

3.4 **Expressed Population Signal**

The “expressed population signal” (EPS) is used to evaluate whether the composite time series captures a representative site signal (McCarroll and Loader, 2004; Wigley et al., 1984). $EPS=(n\times r_{mean})\div[(n\times r_{mean})+ (1-n)]$, where n is the number of trees at the site, and r_{mean} is the mean correlation coefficient among all series. Although an EPS > 0.85 is used to suggest that the composite record accurately represents the mean variance of the population and yields a signal relatively free of noise due to individual variation, an EPS<0.85 does not necessarily indicate that the record is an inaccurate

representation of the population signal (English et al., 2010). For example, English et al. (2010) indicate that the $\delta^{18}O$ values of cactus in South America effectively records the ENSO-relation precipitation, although the EPS of five cactuses of $\delta^{18}O$ is 0.66. Berkelhammer and Stott (2011) reconstruct 500-years temperature in the Rocky Mountains by Bristlecone Pine cellulose oxygen isotope. While EPS value is 0.72, the isotope-based temperature reconstructions show good similarity with both regional wood density-based temperature reconstructions and early instrumental records.

3.5 Climate analysis

The samples of Fokienia at PL were from 1,300 meters in the forested mountains, while the Luang Prabang weather station is below 400 meters. Komonjinda (2003) analyzed elevational temperature/rainfall/relative humidity profiles in northern Thailand and illustrated how poorly low-elevation stations reflect mountain climates. Therefore, The CRU TS3.0 (http://badc.nerc.ac.uk/data/cru/) gridded temperature/precipitation datasets with a resolution of 0.5° × 0.5°, and the gridded Palmer Drought Severity Index (PDSI) series with a resolution of 2.5° × 2.5° (Dai et al., 2004) were used to evaluate the climate sensitivity of tree-ring cellulose $\delta^{18}O$. I produced an average temperature/precipitation and PDSI from the 100 CRU grid points and 4 PDSI grid points, respectively, (17.5°–22.5°N, 100°–105°E) within the study site. The PDSI, which was created by Palmer (1965), is the most popular drought index in the United States. The PDSI was used to measure long-term drought, which lasts for a few months. On the PDSI calculation, Palmer (1965) employed recent precipitation and temperature as input. Because precipitation and temperature are normal climate variables that have long instrumental records, long PDSI records are available based on the long temperature and

precipitation records in some places in the world.

I utilized the KNMI Climate Explorer (http://www.knmi.nl/) to examine the spatial correlation between the oxygen isotope chronology and the SST from the NCDC v3b dataset (Smith et al., 2008). I also examined the spatial correlation between the PL cellulose $\delta^{18}O$ chronology and the SST from the NCDC v3 dataset (Smith et al., 2008) to identify large-scale forcing effects on tree ring cellulose $\delta^{18}O$. For this purpose, I utilized the KNMI Climate Explorer (http://www.knmi.nl/) (van Oldenborgh and Burgers, 2005). The Multivariate ENSO Index (MEI) based on the six main observed variables (sea-level pressure, zonal and meridional components of the surface wind, sea surface temperature, surface air temperature, and total cloudiness fraction of the sky) over the tropical Pacific was used to monitor ENSO (Wolter and Timlin, 2011). High MEI values indicate El Niño events. I compared the PL cellulose $\delta^{18}O$ chronology with the MEI from 1871-2002 to explore the influences of ENSO on local climate (Wolter and Timlin, 2011). The $\delta^{18}O$ data were annual, while the MEI was bi-monthly. Thus, I employed the average value of the MEI from the previous November to the current October as the annual value of the current year.

4 Cross-dating tree-ring chronologies based on variations of oxygen isotope ratios in cellulose

4.1 Difficulty of cross-dating using ring width in study area

The accuracy of tree-ring chronologies based on cross-dating offers a considerable advantage over other natural archives of palaeoclimatic information (Fritts, 1976). Cross-dating (Figure 4.1) matches the pattern of wide and narrow rings between different trees to give the absolute year when each ring formed (Stokes and Smiley, 1968). The similarity in patterns of ring width originates from a common response to external factors (e.g., climate). Cross-dating based on tree-ring width patterns is a key step in the process of developing a tree-ring chronology.

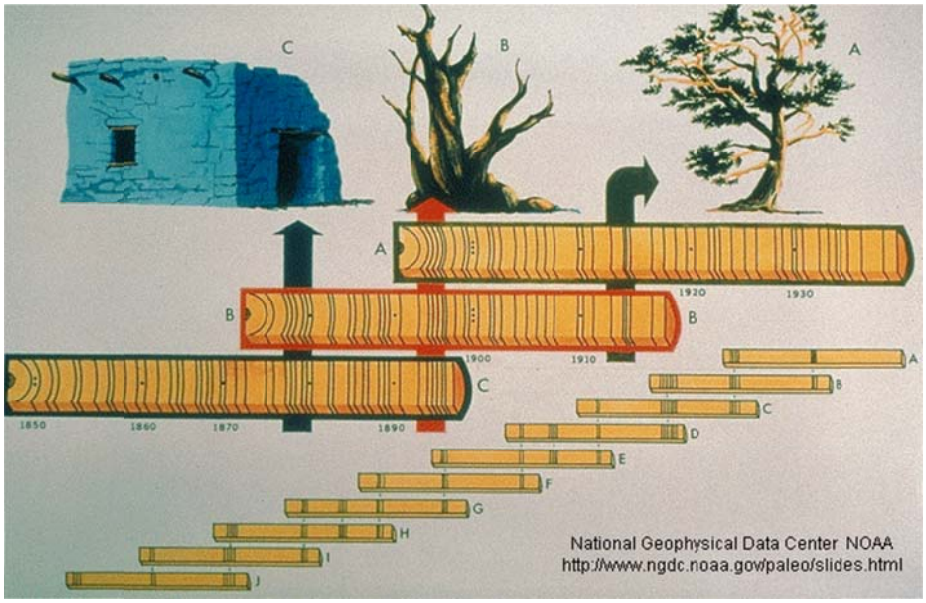

Figure 4.1 The schematic diagram of cross-dating (from NOAA website).

Fokienia hodginsii grows in the mountain regions of Vietnam and Laos and is one of the most suitable tree species to use for reconstructing past climate variability in Southeast Asia (Sano et al., 2009; Buckley et al., 2010). Significantly, this species may live for more than 1000 years, and shows a direct response to hydroclimatic conditions. However, frequent endogenous disturbances caused by the closed-canopy nature of the stands often hinders cross-dating of samples from this species. For example, Sano et al. (2009) reported that more than half of 120 core samples could not be cross-dated. The matching of ring-width patterns from the trees sampled in the present study was also rather difficult. In this paper, PL_{rw} and PL_{o} represent the chronologies derived from the ring width and oxygen isotope data, respectively.

For PL case (this study), only 26 cores from 15 trees (total number of cores is 112) were precisely dated from the period during the period of 1925-2002 in the PL area. Before 1925, the expressed population signal (EPS) (Wigley et al., 1984) of the PL chronology which was developed by ring width is less than 0.85, while the mean inter-series correlation (Rbar) is less than 0.19. The PL tree ring width chronology just provides a robust estimate on mean growth of *Fokienia* during the last 80 years, but the chronology is less reliable before 1920. In practice, I found that ring-width patterns cannot be matched with each other before 1850 using the cross-dating process in the laboratory.

4.2 Cross-dating by tree ring cellulose oxygen isotope

In addition to ring width, variations in stable isotope concentration within the cell structure of the tree ring may also be correlated with environmental parameters (McCarroll and Loader, 2004). The nature of the oxygen isotopes preserved in tree-ring cellulose is mainly controlled by relative humidity and the oxygen isotope composition of the source water (Roden et al., 2000; Robertson et al., 2001). Tree-ring oxygen isotope series usually display higher signal strengths than equivalent ring width and density series (Anderson et al., 1998; Gagen et al., 2011), and are not as strongly affected by the physiological characteristics of individual trees (Raffalli-Delerce et al., 2004; Nakatsuka, 2007). These properties make stable isotopes useful for cross-dating.

Leavitt et al. (1985) were the first to indicate that the isotopic pattern is pronounced and reflects the regional isotopic signal despite its ring-width complacency, and isotopic patterns could provide useful information for dating the undated samples. Roden (2008) used oxygen and carbon isotopes to cross-date redwood that was very hard to be cross-dated by ring-width data because of complacent growth of redwood. By comparing two tree-ring cellulose $\delta^{18}O$ time series, Li (2011) identified missing rings that were not detected by ring width cross-dating. These studies indicate a potential for cross-dating based on stable isotope time series from tree-rings.

To obtain the accurate chronology, I used tree-ring cellulose $\delta^{18}O$ data for cross-dating. In addition, the number of missing rings in the *Fokienia* from the PL area was expected to be very low, because I found only three missing rings in the series dated from 1920. Overall, a total of 12 missing rings were identified by visually examining scatter plots of the oxygen isotope series, while the total number of rings was 1646. Several missing rings emerged next to very narrow rings; however, missing rings from different cores did not occur in the same year. The gaps evident in the tree-ring $\delta^{18}O$ time series (Figure

4.2a) can mostly be related to either the rings being too narrow to produce a large enough sample for oxygen isotopic measurement, or the loss of several rings during the chemical treatment. A visual inspection shows several pointer years in the $\delta^{18}O$ time series in Figure 4.2a (e.g., 1635, 1647, 1662, 1783, 1785, 1877, 1902, 1909, 1920, 1956–1957, 1964, 1971, 1983, 1992, and 1998). The age profile, EPS, and Rbar of the $\delta^{18}O$ time series are shown in Figure 4.2b and 4.2c. The tree-ring $\delta^{18}O$ shows good inter-series correlation among the 7 trees over the past 400 years, as seen in the running Rbar statistics (0.46–0.69) calculated using 50-year windows and a lag-time of 25 years. The EPS for the $\delta^{18}O$ remained above 0.8 from 1620 onwards.

Although our analysis indicates the statistical reliability of the PL_o chronology which was developed by tree ring cellulose $\delta^{18}O$ (Figure 4.2c), it is clearly preferable to test the accuracy of the chronology using another validation method because this is the first attempt at establishing a long tree-ring chronology using only $\delta^{18}O$ series. Sano et al. (2009) established a ring-width chronology spanning 535 years at the MCC site located 150 km northeast of our PL site. The reliability of the MCC_{rw} chronology allowed us to test the accuracy of the PL_o chronology by comparing it with the MCC oxygen isotope chronology (MCC_o chronology: Figure 4.3, blue line) (Sano et al., 2012). The correlation between the two $\delta^{18}O$ chronologies was highly significant ($r = 0.70$, $n = 298$) and relatively stable over most of the last 300 years (Figure 4.3b). The strength of the correlation fell in the periods 1930–1950 and 1830–1850, which also coincided with a decrease in Rbar in the PL_o chronology. Nevertheless, the fluctuations and marker years of both chronologies show similar characteristics. In particular, the pattern of an extremely high value in 1783, followed by a very low value in 1785, is clearly identifiable in both series, and could be used as a tight-point to cross-date other samples in this area.

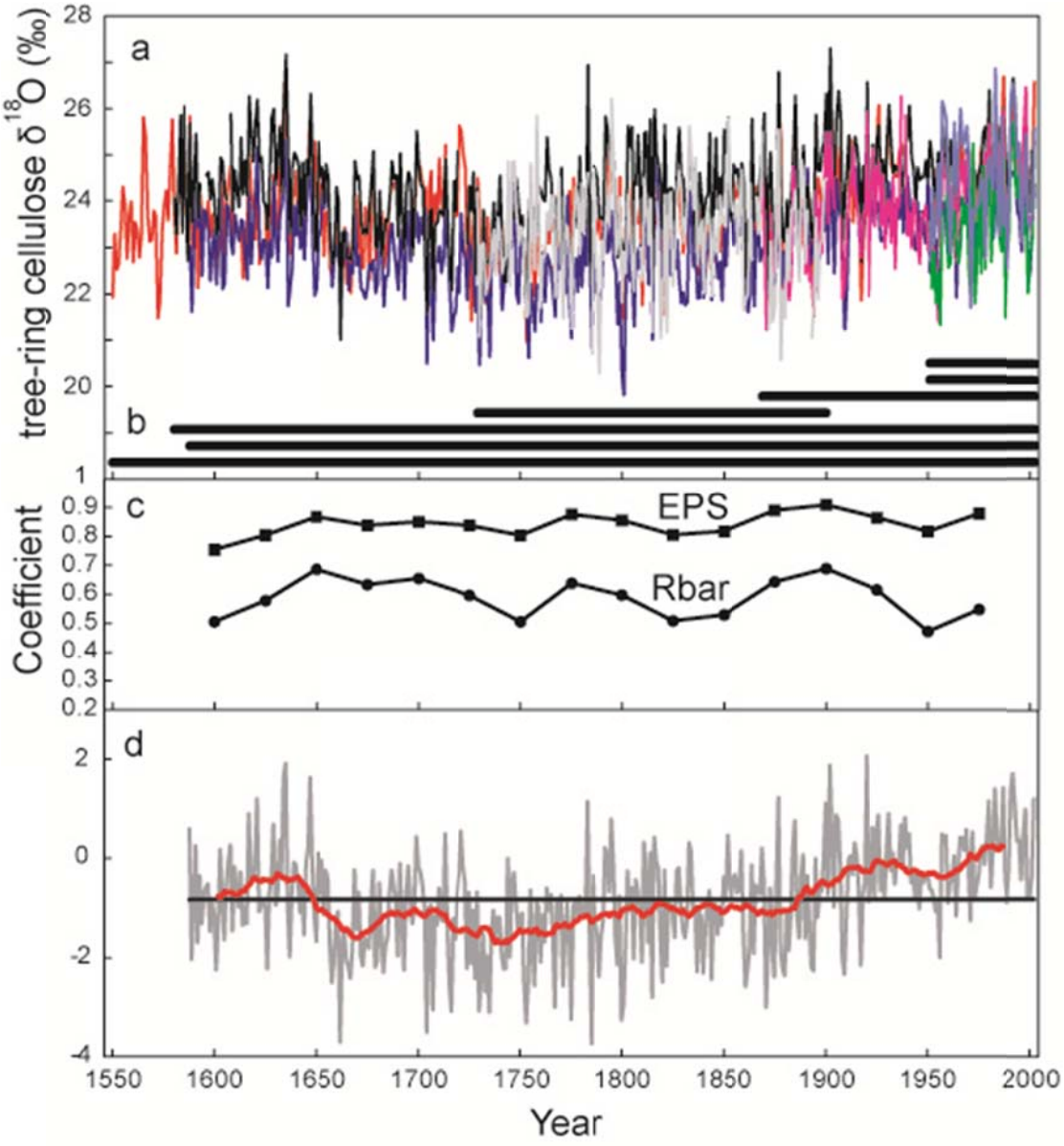

Figure 4.2 a: Tree-ring $\delta^{18}O$ series of 7 trees, b: age profile, c: its running EPS and Rbar statistics used 50-year windows, lagged 25 years, d: normalized $\delta^{18}O$ chronology (gay line), mean value (black line) and 31 running average (red line).

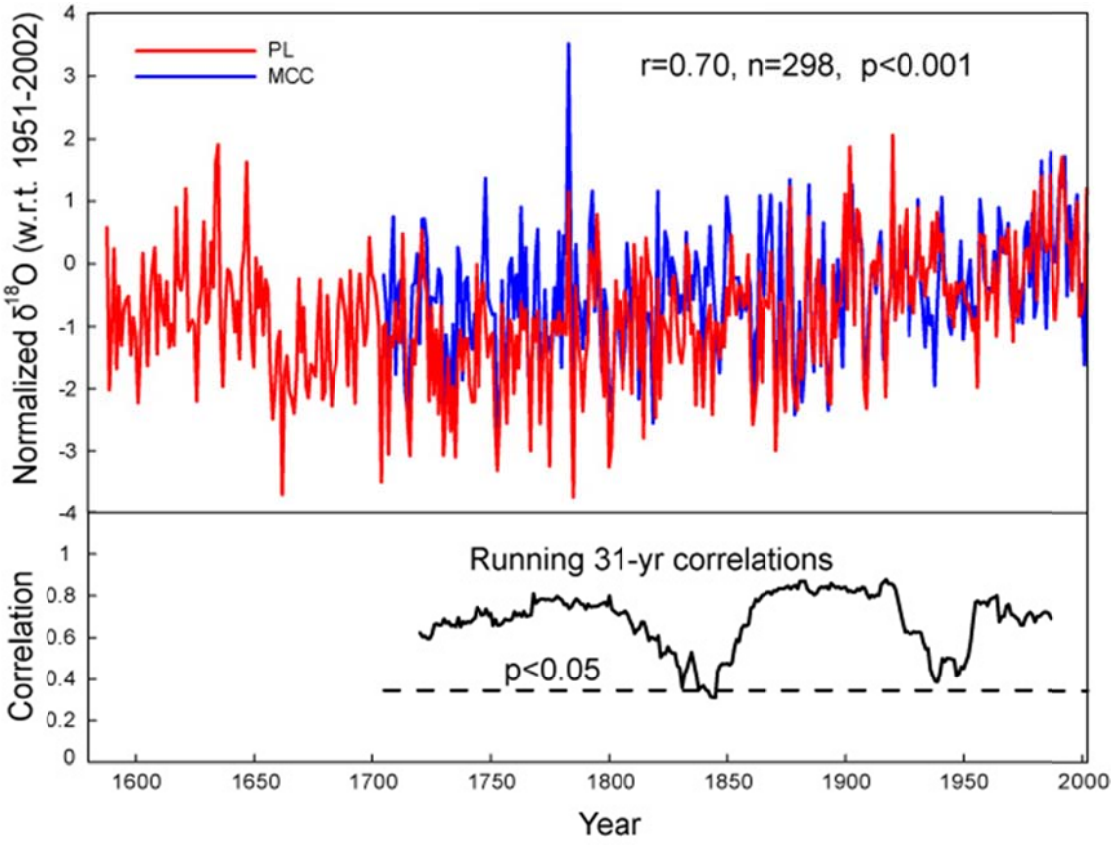

Figure 4.3. a: Time series of PL_o chronology (red line) and MCC_o chronology (blue line), b: Running 31-year correlation between PL_o and MCC_o.

In addition, I used the COEFCHA program to evaluate the quality of the cross-dating derived from the oxygen isotope data. Based on the good correlation between the MCC_o and PL_o chronologies, 7/6 oxygen isotope time series from PL/MCC were run through COEFCHA together. A 50-year segment length with a 25-year overlap was used for correlations test. I used a 32-year spline (without autoregressive modeling and log transformations) to remove the low frequency signal. For the PL_o chronology, there were three A flags (correlation under 0.3281 (99% confidence) but highest during the 21 years), and one B flag (correlation is highest but at other dated position), while the total number of segments was 68. Consequently, I believe that the PL_o chronology is reliable, and offers an alternative approach for dendrochronologists at sites where cross-dating using tree-ring widths is not possible, such as PL.

4.3 Developing tree ring cellulose oxygen isotope chronology

Due to differences in the average $\delta^{18}O$ values between cores, calculating mean values from all of the raw time series to build the chronology may result in some artificially abrupt increases in $\delta^{18}O$ values in the years where cores end or begin. Therefore, six oxygen isotope time series were individually normalized over the entire time period based on the common period 1951–2002. For PL107a, which does not cover this common period, the z-scores are calculated from $Z_t = (x_t – m_x)/s_x$, where x_t represents the values of $\delta^{18}O$ in year t, and m_x and s_x are the average of the mean and standard variation, respectively, of the other six cores between 1951 and 2002. The seven series were then averaged to produce the final $\delta^{18}O$ chronology for the period 1588–2002 (Figure 4.3a, red line).

The EPS values from certain sections of the PL_o chronology are lower than 0.85, which is the generally accepted threshold value (McCarroll and Loader, 2004). To test the effect of EPS on the accuracy and climate sensitivity of the oxygen isotope chronology, I compared the PL oxygen isotope chronologies derived from four and six cores in the period 1951–2002. Xu et al. (2011) used four cores to develop an oxygen isotope chronology at PL from 1951 to 2002 that had an EPS value of 0.80. In this study, I developed an additional oxygen isotope chronology by adding two more cores from 1951 to 2002, and this had an EPS value of 0.88. For convenience, I refer to them as the PL4 and PL6 chronologies. As shown in Tables 4.1 and 4.2, PL4 and PL6 have non-significant differences in their correlations with the MCC_o chronology and climatic parameters, although the EPS of PL4 is 0.80. Can an EPS of 0.80 be considered adequate for an oxygen isotope chronology in the PL area? Noise

within oxygen isotope data originates mainly from analytical errors related to technical processes, such as the stability of the mass spectrometer and/or the cutting accuracy of samples at ring boundaries, while noise associated with ring width arises from endogenous ecological disturbance. Therefore, averaging several oxygen isotope time series can reduce noise and provide a robust chronology, even the EPS is less than 0.85. If 0.8 is accepted as a suitable EPS threshold for oxygen isotope chronologies, then our PLo chronology is robust from 1620 to 2002.

Previous studies show that age-related long-term decreasing trends exist in tree-ring $\delta^{18}O$ time series (Treydte et al., 2006; Nakatsuka, 2007; Esper et al., 2010). However, our $\delta^{18}O$ time series shows no significant trend between 1550 and 2002. It should be noted that two of the three longest cores (red and black lines in Figure 3a) extend to 1520, and there is even an increasing trend between 1550 and 1650, which is the opposite of previous findings (Treydte et al., 2006; Nakatsuka, 2007; Esper et al., 2010). In addition, a recent study indicates that aging effects on oxygen isotope series are not seen in tree-rings whose cambial ages exceed 50 years (Young et al., 2011). Therefore, it is reasonable to assume that the aging effect does not significantly affect our $\delta^{18}O$ time series.

For the PL site, tree-ring oxygen isotope data provided a robust chronology covering 380 years, while the ring-width chronology was only able to cover a period of 80 years. The main reason for this discrepancy is that tree-ring oxygen isotope levels are not as strongly affected by the physiological characteristics of individual trees as ring widths are. Nakatsuka (2007) analyzed oxygen isotopes from three Larix trees in Far East Russia. Although ring-width patterns from these trees were less well correlated with one another, he found a remarkable consistency in their oxygen isotope time series. In addition to this advantage, inter-species tree-ring cellulose δ18O series still show very similar variations (Li et al., 2011). Furthermore, within the same climatic zone, oxygen isotope chronologies that are 200–1000 km apart also

show similar variations (Nakatsuka, personal communication). Such advantages associated with the use of oxygen isotope series make them a promising tool for cross-dating at both the local and regional scale.

Because obtaining oxygen isotope data is a time- and cost-consuming work, this isotope approach will not replace traditional ring-width analysis at sites where the traditional tree-ring proxies (ring width, density) already are suitable for cross-dating and paleoclimate reconstruction. Based on the precondition that the proportion of missing rings is low, I suggest that oxygen isotope series should be used for cross-dating if either cross-dating by ring width does not perform well due to the absence of a dominant external limiting factor or frequent endogenous disturbance, or if the number of samples is limited (e.g., archeological samples).

Table 4.1 Correlation between PL4/PL6 chronology and temperature, precipitation, and PDSI.

r	p-Nov	p-Dec	Jan	Feb	Mar	Apr	May	Jun	Jul	Aug	Sep	Oct.	May-Oct
Temperature-PL4	-0.06	0.21	0.08	0.00	0.21	0.27*	0.62**	0.40**	0.49**	0.30*	0.21	0.12	0.66**
Temperature-PL6	-0.06	0.21	0.15	0.03	0.25	0.24	0.56**	0.41**	0.48**	0.32*	0.15	0.16	0.64**
Precipitation-PL4	-0.16	-0.17	0.17	0.15	0.00	-0.22	-0.43**	-0.15	-0.04	-0.20	-0.12	-0.26	-0.48**
Precipitation-PL6	-0.10	-0.17	0.15	0.19	-0.01	-0.17	-0.42**	-0.14	-0.02	-0.13	-0.13	-0.25	-0.43**
PDSI-PL4	-0.21	-0.24	-0.23	-0.26	-0.35*	-0.51**	-0.63**	-0.59**	-0.59**	-0.66**	-0.60**	-0.59**	-0.66**
PDSI-PL6	-0.23	-0.19	-0.27*	-0.29*	-0.38**	-0.52**	-0.62**	-0.59**	-0.59**	-0.64**	-0.61**	-0.60**	-0.64**

*p < 0.05; **p < 0.01

Table 4.2 Rbar and EPS of PL4/PL6 oxygen isotope chronology, and their correlation with the MCC oxygen isotope chronology.

	Rbar	EPS	R with MCC
PL4	0.51	0.80	0.77
PL6	0.55	0.88	0.77

5 Intra-annual variations of tree ring oxygen isotopes for trees without distinct rings

5.1 The purpose of intra-annual tree ring oxygen isotopes research

Tropical trees often fail to develop reliable annual rings, because most trees do not have visible rings or just have indistinct ring. Therefore, estimating the growth rate and age of tropical trees is a very difficult work, which not only can provide the essential information to understand the forest dynamics and evaluate the forest response to global change, but also help to reconstruct climate in the past. Therefore, identification annual growth for trees with non-distinct ring pattern becomes very important. Dendrometer can measure radial growth rate of tropical trees by continuous measurement of diameter growth (da Silva et al., 2002; Ohashi et al, 2005). However, the dendrometer method cannot provide the growth rate of tree before the marking period.

Another method to measure growth of trees is to detect of periodicity of wood formation. Tree ring oxygen cellulose isotopes are mainly controlled by that of soil water and relative humidity (Roden et al., 2000). In tropical area with distinct rainy and dry season, $\delta^{18}O$ of precipitation and relative humidity usually show clear seasonality. Oxygen isotope of precipitation usually has a negative correlation with rainfall (amount effect) (Dansgaard, 1964; Araguas-Araguas et al., 1998) in tropical area. Rainy season in the tropics is characterized by ^{18}O depleted precipitation water, and high relative humidity

which usually appear in rainy season result in lower tree ring cellulose oxygen isotopes. Such the seasonal cycles of $\delta^{18}O$ of precipitation and relative humidity finally generate seasonal cycle of tree ring $\delta^{18}O$ which is helpful to identify annual growth. If I analyze samples with a sufficiently high radial resolution, seasonal cycle of tree ring $\delta^{18}O$ can be caught (Evans and Schrag, 2004; Poussart et al., 2005; Anchukaitis et al., 2008 and 2010).

In this study, I simulate tree ring $\delta^{18}O$ data based on fractionation model (Sternberg, 2009), and compare modeled tree ring $\delta^{18}O$ data with measured tree ring $\delta^{18}O$ data from two cores of *Ficus* in a seasonally dry forest and one disk of *Styrax* in a seasonally dry plantation (KA site in Figure 3.1) in Laos to 1) further investigate the potential of the use of tree ring cellulose $\delta^{18}O$ for measuring annual growth of trees without distinct rings, 2) cross-check the periodicity between different species.

5.2 Forward modeling for tree ring $\delta^{18}O$ data

I hypothesize that the isotope of precipitation and relative humidity difference between wet season and dry season is enough to generate annual cellulose oxygen isotope cycles in trees. I use the Sternberg. (2009) model (Eq.(5)) of the environmental controls on the tree ring cellulose oxygen isotope to simulate a modeled tree ring $\delta^{18}O$ record based on relative humidity and precipitation $\delta^{18}O$ from meteorological station. Modeled tree ring $\delta^{18}O$ record is then compared with measured tree ring cellulose $\delta^{18}O$ record from *Ficus sp* and *Styrax* to detect if annual cycles of oxygen isotopes exist. The tree ring $\delta^{18}O$ model (Eq.(5), Sternberg. 2009) can be used to calculate tree ring cellulose oxygen isotope under one important assumption: $\delta^{18}O$ of precipitation is equal to $\delta^{18}O$ of source water (xylem water).

5.2.1 Model parameters

The equilibrium (ε*) /kinetic (ε_k) fractionation factor that are derived from previous study (Allison et al., 1995) are about 29‰ and 19‰, respectively. The proportion of oxygen isotope exchange between xylem water and oxygen in organic matter (f_o) do not change with different temperatures (Sternberg and Ellsworth, 2011), I adopt previously reported 0.42 as f_o value for calculation purposes (Roden et al., 2000; Sternberg and Ellsworth, 2011). Although ε_o (the biological isotopic fractionation factor between oxygen in organic matter and oxygen in xylem water) is temperature-sensitive, ε_o changed a little within temperature from 20ºC to 30ºC (Sternberg and Ellsworth, 2011). Monthly temperature fell range from 18ºC to 26ºC in our sampling site. 27‰ has been observed in previous studies (Sternberg et al., 1984; Sternberg and DeNiro 1983; Yakir and DeNiro, 1990). Therefore, I employed 27‰ as ε_o value in the model. For the fraction of enriched water (α), 67% to 90% values were reported (Allison et al., 1985; Flanagan et al., 1991; Roden et al., 2000). In this study, relative humidity in the sampling sites (PL) are relatively high, therefore evapotranspiration are not very strong in growing season at wet mountainous regions, then the Péclet effect does not seem to exert strong influences on the leaf water $\delta^{18}O$, and then I assume α is equal to 80% for calculation.

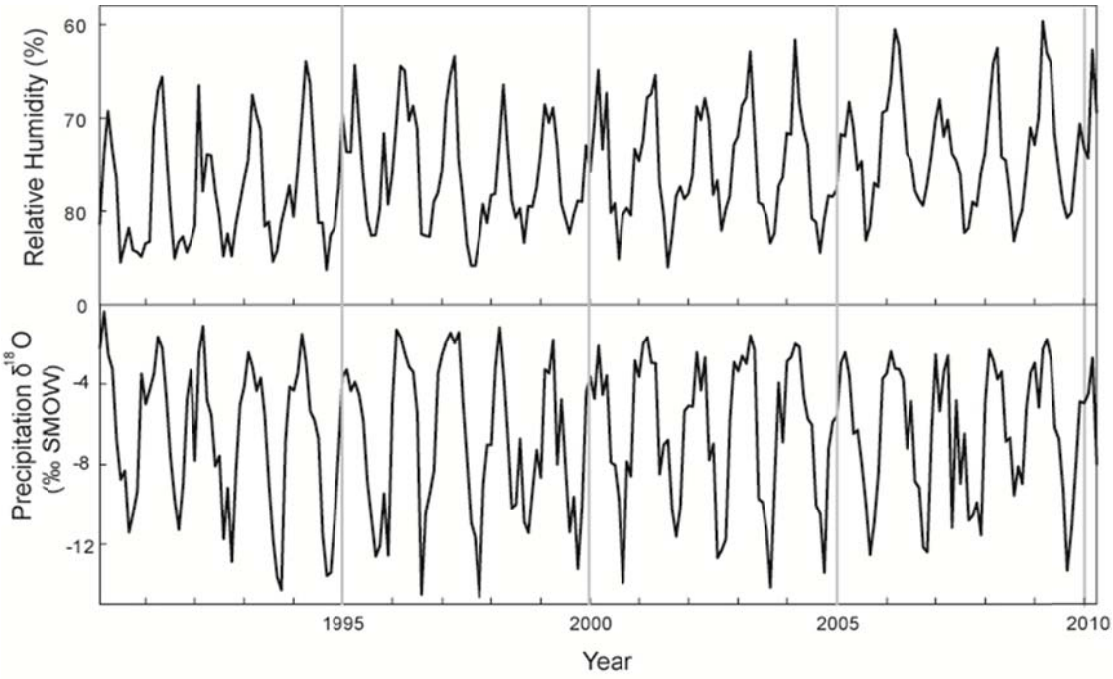

Figure 5.1 Input data (Relative humidity and Precipitation $\delta^{18}O$ time series) for tree ring $\delta^{18}O$ model (Yoshimura et al., 2008)

5.2.2 Input data and modeled tree ring $\delta^{18}O$

Based on Eq.(5) (Sternberg 2009), input data are monthly oxygen isotopes of precipitation and relative humidity (Figure 5.1a). Monthly oxygen isotope of precipitation data is derived from an isotope-enabled atmospheric model simulation IsoGSM (Yoshimura et al., 2008). I averaged data from two sites which are nearest grid points with sampling site (20°N, 101.25°N; 20°N, 103.125°N). Monthly relative humidity data is from the Muang Xai weather station (20. 69°N, 101. 98°E). Simulated tree ring data by oxygen isotope model are shown in Figure 5.2. Modeled monthly tree ring $\delta^{18}O$ produce clear annual cycles during the period 1990-2010, and the mean amplitude of modeled $\delta^{18}O$ is 11.4‰.

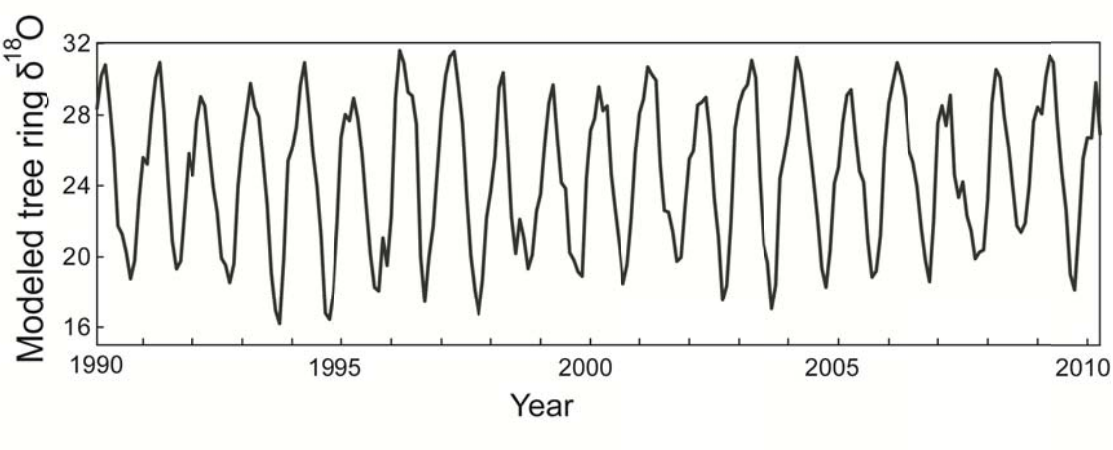

Figure 5.2 Modeled tree ring $\delta^{18}O$ time series

5.3 Comparisons between measured and modeled tree ring $\delta^{18}O$

The sample of *Styrax* (Figure 5.3a) had a distinct annual cyclicity of $\delta^{18}O$ values, and had a mean $\delta^{18}O$ of 22.96‰. Minima and maxima in $\delta^{18}O$ could be distinguished with mean amplitude of 8.7‰. These is a slightly decrease trend of maxima in $\delta^{18}O$ of *Styrax.* The mean $\delta^{18}O$ of two *Ficus* cores (Ka018, Ka019) were 24.22‰ and 24.42‰, and mean amplitude of $\delta^{18}O$ cycles were 4.8‰ and 5.1‰, respectively (Figure 5.3b & c). No obvious longer-term trend in $\delta^{18}O$ could be distinguished in the *Ficus* cores.

In order to produce continuous tree ring $\delta^{18}O$ time series, I develop a simple age model for the tree ring $\delta^{18}O$ by pattern match method, which is based on tree ring cellulose oxygen isotope model results (Figure 5.2). Previous studies (Anchukaitis et al., 2008; Zhu et al., 2012) employed the similar method to assign time to intra-annual oxygen isotope record. In detail, I assigned the cellulose $\delta^{18}O$ maxima of each cycle of tree samples to the month which has

modeled highest tree ring $\delta^{18}O$ value in a year, and the cellulose $\delta^{18}O$ minima of each cycle to the month which has modeled lowest tree ring $\delta^{18}O$ value in a year.

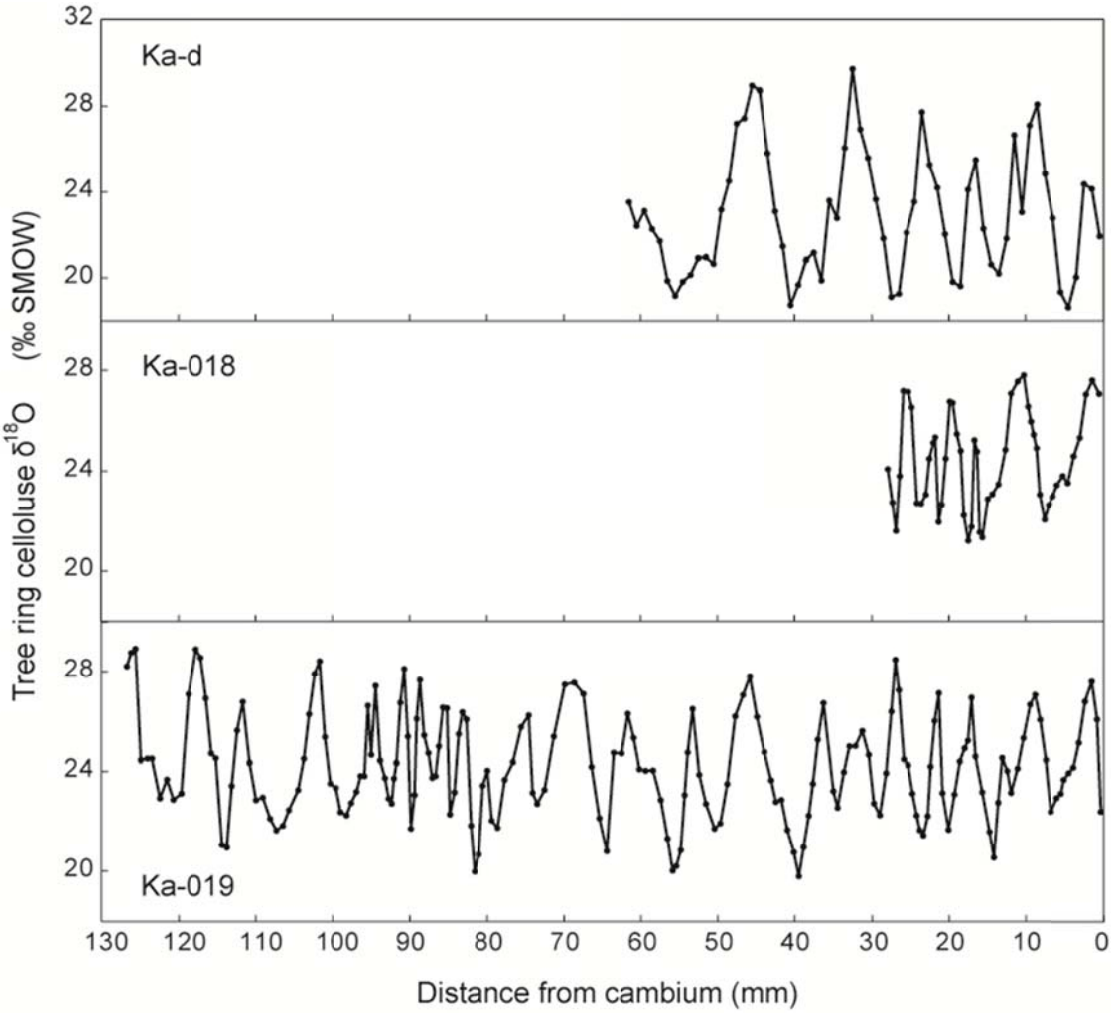

Figure 5.3 Intra-annual variations of tree ring $\delta^{18}O$ of Ka-d (*Styrax*), Ka018 and Ka019 (*Ficus*).

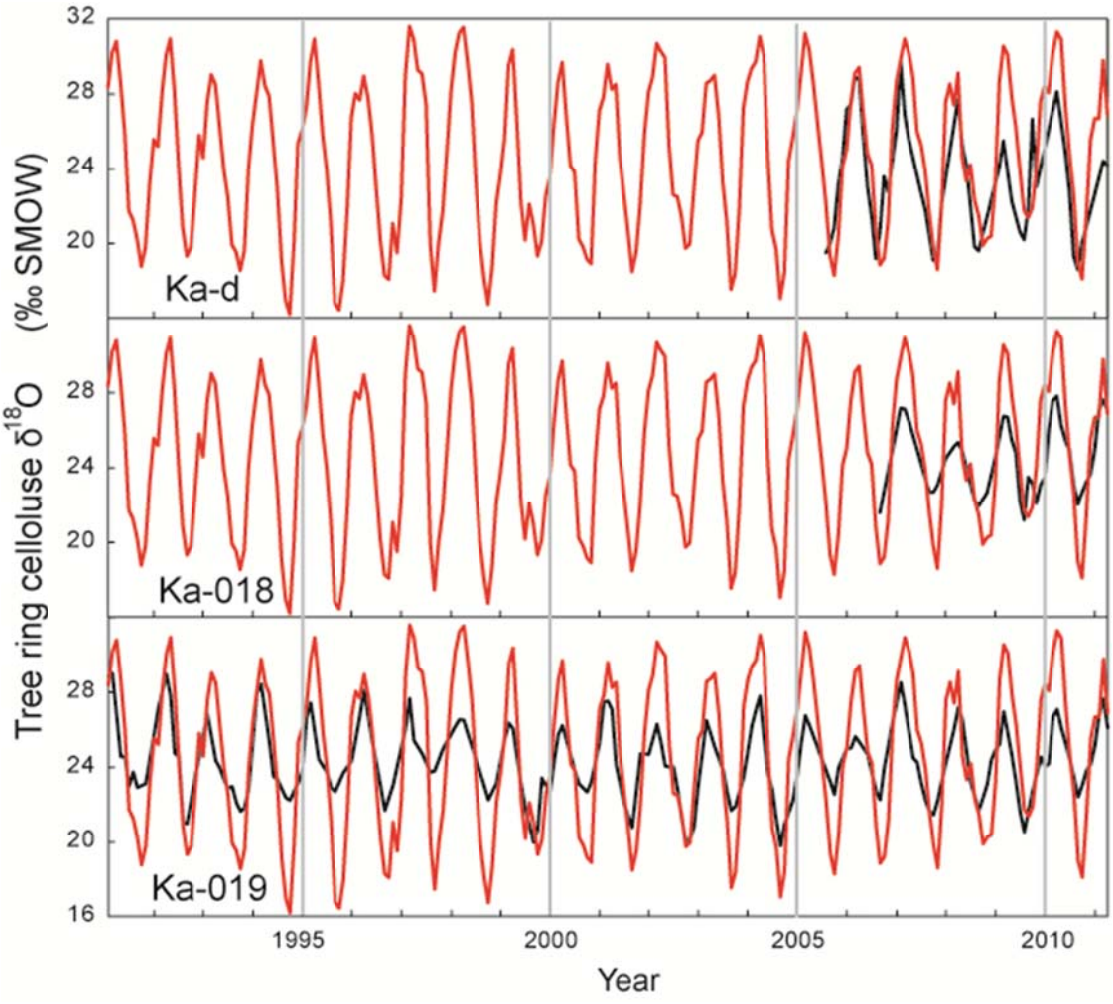

Figure 5.4 Modeled (red line) and measured (black line) tree ring $\delta^{18}O$ time series

From these key points, adjacent samples are linearly interpolated by one sample per month. While modeled peak tree ring $\delta^{18}O$ value in one year usually appears in February/March, modeled lowest value is in August/September. Age models were developed individually for every tree

samples (Figure 5.4). The mean inter-series correlation between the monthly $\delta^{18}O$ series for the three trees is 0.81. The correlation between two cores of *Ficus* (Ka-018 & Ka-019) is 0.87. Annual growth of *Styrax* calculated based on the age modeled $\delta^{18}O$ chronologies revealed reduction in growth rate, which should be considered as juvenile effect.

The cyclic variation in $\delta^{18}O$ of *Styrax* over distances (Figure 5.3a) suggests a forcing by seasonally varying environmental conditions. There are six clear $\delta^{18}O$ cycles, while *Styrax* is 7 years old. Considering germination time, $\delta^{18}O$ cycles of *Styrax* which are shown in Figure 5.3a are considered as annual cycles. $\delta^{18}O$ cycles of *Ficus* show similar features with $\delta^{18}O$ cycles of *Styrax*, although amplitude of *Ficus* samples is a little smaller than *Styrax* sample. Therefore, I infer that $\delta^{18}O$ cycles of *Ficus* are annual cycles. The formation of tree ring annual $\delta^{18}O$ cycles are derived from local climate situation (distinct wet/dry season). Based on tree ring cellulose oxygen isotope theory (chapter 2), precipitation $\delta^{18}O$ and relative humidity are two main factors to control the tree ring cellulose $\delta^{18}O$. In rainy season, both low precipitation $\delta^{18}O$ result from heavy rainfall (amount effect) and high relative humidity (weak evapotranspiration) result in lower tree ring cellulose $\delta^{18}O$ (Eq.(5) in chapter 2), vice versa.

The mean of $\delta^{18}O$ *Styrax* is about 1.3‰ lower the value of *Ficus sp*, while the annual amplitude of $\delta^{18}O$ *Styrax* is about 3.5‰ higher the value of *Ficus sp*. I can infer that the following reasons cause these differences. Firstly, *Styrax* is relative young and its shallow root system takes upper soil water, while *Ficus sp* is older than *Styrax* and its relative deep root system take soil water from middle or lower part of soil profile. Although I do not know the exact age of *Ficus sp*, I infer that age of *Ficus sp* at least older than 20 based on counting oxygen isotopes annual cycles. $\delta^{18}O$ of soil water study in Southwest China shows that amplitude of $\delta^{18}O$ of precipitation, soil water in 50cm and 100cm are 0‰ to -10‰, -2‰ to -9.3‰ and -2.7‰ to -8.3‰, respectively (Luo and Wang, 2008). There is a decrease trend of amplitude of $\delta^{18}O$ soil water with

depth of soil profile, which was brought by a mixture process of different periods and event's precipitation. Therefore, annual amplitude of *Styrax* with relative shallow root system is higher. Secondly, leaf morphology has an effect on Peclet effect which is related to leaf water enrichment. *Ficus sp* and *Styrax* has different leaf morphology, which may lead to difference of mean between two species.

The correlations between monthly modeled cellulose $\delta^{18}O$ and monthly observed $\delta^{18}O$ of Ka-d (*Styrax*), Ka018 and Ka019 (*Ficus*) are 0.79, 0.77 and 0.84, respectively. The mean of modeled $\delta^{18}O$ is 24‰, which is closed to observed $\delta^{18}O$. However, the mean amplitude of modeled $\delta^{18}O$ is 11.4‰, which is higher than observed $\delta^{18}O$. The main reason that causes the differences may be derived from our assumption: $\delta^{18}O$ of precipitation is equal to $\delta^{18}O$ of source water. There are two cases that $\delta^{18}O$ of precipitation is not equal to $\delta^{18}O$ of source water will cause the differences between modeled and measured data. One is that not only new precipitation $\delta^{18}O$ but also the previous month's precipitation $\delta^{18}O$ will control soil water $\delta^{18}O$. Because precipitation water in soil has long residence times, these would result in mixing of precipitation water from different months, and finally amplitude of annual soil water oxygen isotope would be dampen. Therefore, mixing of precipitation from different months in the soil leads to the smaller annual amplitude of the soil water /tree ring cellulose $\delta^{18}O$. Previous tree ring cellulose $\delta^{18}O$ modeling study in Costa Rica also shows that a soil water-mixing model (70% of the previous months' soil water mixing with 30% current precipitation) will achieve the best match between annual amplitude in the simulated and actual tree ring $\delta^{18}O$ records (Anchukaitis et al., 2008). In addition, if trees absorb not only rainwater but also underground water, the amplitude of xylem water $\delta^{18}O$ annual cycle will be smaller than the amplitude of precipitation $\delta^{18}O$ annual cycle.

However, monthly modeled cellulose $\delta^{18}O$ and monthly observed $\delta^{18}O$ of Ka-d (*Styrax*) (Figure 5.4) during the first three years fit very well each other.

This seems to support our assumption. But annual amplitude of modeled cellulose $\delta^{18}O$ is higher than amplitude of observed $\delta^{18}O$ of Ka-d (*Styrax*) after the tree germinate three years, because root become deeper than trees utilize the soil water in deeper part of soil profile. Therefore, the difference of annual amplitude between modeled and observed cellulose $\delta^{18}O$ (ka 018&019, *Ficus*) (Figure 5.4) may originate from deeper root system of *Ficus* trees.

5.4 The potential of intra-annual variations of tree-ring cellulose $\delta^{18}O$

Tree ring $\delta^{18}O$ modeling results independently supports our detection of oxygen isotopes annual cycles. Therefore, tree ring cellulose oxygen isotope have great potential to identify the annual growth for tropical trees without distinct annual rings in the context of seasonal climate, which is essential information for forest management and dendrochronological research.

6 Hydroclimate variability in northern Southeast Asia during 1588-2002

6.1 Tree-ring width and $\delta^{18}O$ chronology

Table 6.1a presents the correlation coefficients (r) among ring width time series. The mean inter-tree correlation coefficients of ring width is 0.32 (n=52, 6 series). The ring width standard chronology (STD chronology) which contain 26 samples was established by ARSTAN program (Cook et al., 1985) from 1920.

The individual tree-ring cellulose $\delta^{18}O$ time series and composite chronology are shown in Figure 4.2. The mean $\delta^{18}O$ values of 6 trees calculated for the common period of 1951–2002 range from 23.39‰ to 24.88‰. The inter-tree variability for $\delta^{18}O$ exhibited a range of 0.3-2‰, and the typical inter-tree variability for $\delta^{18}O$ summarized by *Leavitt* (2010) fell within the range of 1-4‰. The mean $\delta^{18}O$ values are 1.0–1.3‰ higher than those obtained from 6 trees of *Fokienia hodginsii* in northern Vietnam (Sano et al., 2012). Due to the lower latitude/elevation of our sampling site, $\delta^{18}O$ of precipitation (source water) is expected to be more riched at our site than at the Vietnam site. The standard deviations for each year, calculated after adjusting the mean $\delta^{18}O$ values to 0, exhibit a range of 0.15‰–1.32‰ (mean: 0.57‰), which is comparable to 0.28‰–1.18‰ (0.64‰) computed from the 6 trees from northern Vietnams (Sano et al., 2012).

Table 6.1b presents the correlation coefficients (r) between the different cores. The mean inter-tree correlation coefficients of $\delta^{18}O$ is 0.55 (n=52, 6 series),which is higher than mean inter-tree correlation coefficients of ring

width. This The isotopic records of teak in the India subcontinent exhibit higher mutual coherence than the ring-width records (Managave et al., 2011). Stable isotopes usually display higher signal strengths in comparison to equivalent ring width and density series (Gagen et al., 2011a).

The mean auto-correlations (one year lag) of four cores for ring width and tree-ring cellulose $\delta^{18}O$ are 0.389 and 0.129, respectively. This high autocorrelation of ring width may suggest that tree growth is strongly affected by physiological factors (*Fritts*, 1976). However, the autocorrelation of the tree-ring cellulose $\delta^{18}O$ is low.

An increasing trend (since 1950) is observed in the mean tree-ring cellulose $\delta^{18}O$ series calculated by a linear regression as 0.15‰/decade, which indicates that the monsoon season in this area has become drier. Our results are consistent with the results of Singhrattna et al. (2005), which suggested that the temperature and precipitation exhibit an increasing and decreasing trend, respectively, in the monsoon seasons of the last fifty years in central Thailand. The tree ring cellulose $\delta^{18}O$ in the Asian monsoon area (southeast Tibetan Plateau (Shi et al., 2011), Nepal Himalaya (Sano et al., 2010) and North China (Li et al., 2011b)) reveals a similar trend during the last fifty years.

Table 6.1 Correlation coefficients among time series of ring width (a) and $\delta^{18}O$ (b)

a

r (ring width)	PL101a	PL107a	PL126a	PL136b	PL104b
PL107a	0.433*				
PL126a	0.334*	0.279*			
PL136b	0.186	0.249	0.135		
PL104b	0.192	0.373**	0.407**	0.66**	
PL108a	0.286*	0.177	0.356*	0.331*	0.41**

* p<0.05, ** p<0.01, n=52

b

r ($\delta^{18}O$)	PL101a	PL107a	PL126a	PL136b	PL104b
PL107a	0.504**				
PL126a	0.485**	0.598**			
PL136b	0.346*	0.511**	0.346*		
PL104b	0.568**	0.819**	0.63**	0.529**	
PL108a	0.614**	0.564**	0.558**	0.521**	0.647**

* p<0.05, ** p<0.01, n=52

6.2 Correlation between ring width/$\delta^{18}O$ chronology and climate

Correlation analyses were carried out between tree ring width indices (TRWi), tree-ring cellulose $\delta^{18}O$ and climatic factors (Figure 6.1). All the data are from the common period of 1951–2002. For TRWi, there is a positive relationship with precipitation from the previous October to current March and a negative relationship with monsoon-associated precipitation (May-September). The correlation coefficient between TRWi and precipitation in pervious December is 0.35. TRWi accounts for only 12% of the actual precipitation variance. The TRWi was negatively correlated with temperature from February to May and positively correlated with temperature in August and September (Figure 6.1a). The correlation coefficient between TRWi and temperature in February is -0.28. Buckley et al. (2007a) obtained similar correlations using *Pinus merkusii* in the neighborhood of Vientiane, the capital of Laos. TRWi shows a weak relationship with PDSI.

The relationship between TRWi and climate (Figure 6.1a) suggest that wet conditions in the pre-monsoon period (March to May) are conducive for tree growth. Considering the negative relationship between ring width and precipitation in the monsoon season and the low mean daily sunshine duration in June, July and August, dense cloud cover in summer may limit photosynthesis activity, resulting in narrower rings (Buckley et al., 2007b; Fritts, 1976). The tree ring will be very narrow when spring drought and flood summer happen in one year. In addition, the TRWi are weakly correlated with PDSI. However, the TRWi of teak in northwestern Thailand (Buckley et al., 2007a) and *Fokienia* in northern Vietnam (Sano et al., 2009) showed a positive relationship with pre-monsoon PDSI. The effects of climate fluctuations on tree growth are site-specific (Spiecker et al., 1996). The sampled trees originate

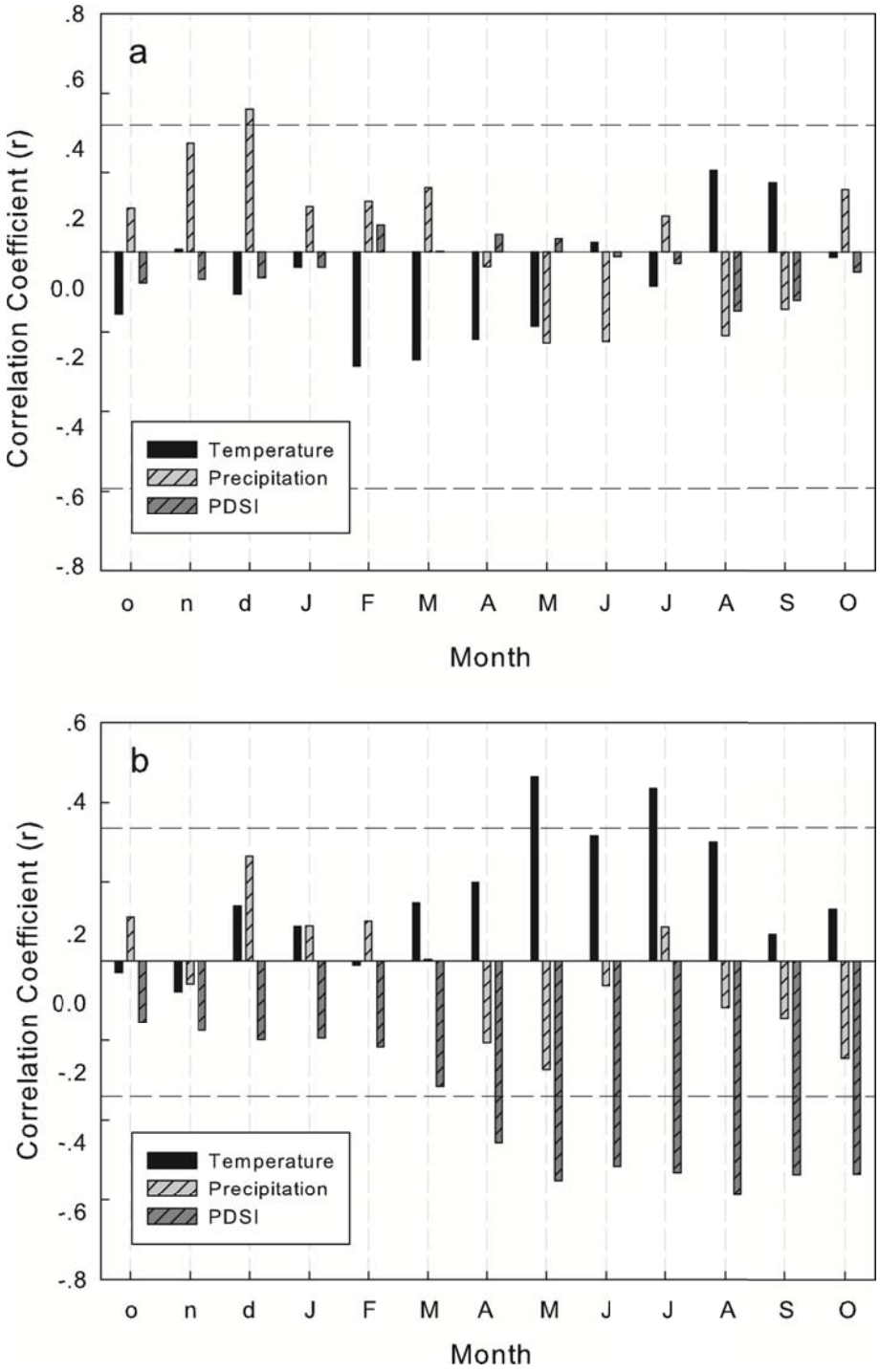

Figure 6.1 Correlation coefficients (r) among (a) temperature, precipitation, PDSI, and TRWi and (b) tree ring cellulose $\delta^{18}O$ of *Fokienia hodginsii*. Horizontal dotted line indicates 99% confidence level, and the lowercase letters indicate (left to right) the previous October, November, and December.

from a closed-canopy forest site, where frequent endogenous disturbance is common, resulting in reduced climate sensitivity. On the whole, tree ring width chronology in sampling site has weak statistical association with climatic parameters, but tree ring width chronology provides for excellent age control which is important for building up precise $\delta^{18}O$ time series and information on tree growth.

Tree-ring cellulose $\delta^{18}O$ (Figure 6.1b) shows significantly positive correlations with temperature from May to August ($r=0.64$, $p<0.001$, $n=52$) and negative correlations with precipitation in May ($r=-0.34$, $p<0.05$, $n=52$). There is a significantly negative relationship between tree-ring cellulose $\delta^{18}O$ and PDSI from May to October ($r=-0.66$, $p<0.001$, $n=52$). Tree-ring cellulose $\delta^{18}O$ accounts for 41% and 44% of the actual temperature from May to August and monsoon season PDSI variance, respectively.

The correlation analyses indicate that the temperature and PDSI of the monsoon season have an important effect on tree-ring cellulose $\delta^{18}O$. In the monsoon season, high temperature usually indicates less rainfall and low relative humidity, which can make the tree-ring cellulose $\delta^{18}O$ heavier. It is easy to understand the significantly negative correlation between the tree-ring cellulose $\delta^{18}O$ and PDSI from Eq. (5). A low PDSI indicates a dry condition. Low soil moisture could result in the evaporation of soil water, so the source water that tree roots take up becomes heavier. However, low relative humidity leads to intense evapotranspiration, which causes the oxygen isotopes of leaf water to be enriched (Roden et al., 2000). That tree-ring cellulose $\delta^{18}O$ has highly negative correlations with the monsoon season PDSI suggests that the trees in study area grow mainly in the monsoon season. A previous dendrometer study on teak in northern Thailand (Buckley et al., 2001) showed that the circumference increased following rain events, particularly during the wet season. Poussart and Schrag (2005) estimated seasonal and annual growth rates by oxygen and carbon isotopes and found that approximately 60% of the annual growth of several evergreen species occurred during the rainy

season (May to October). In addition, tree-ring cellulose $\delta^{18}O$ has a weak relationship with the climate of the previous winter, which indicates that the climate in the previous winter exerts little influence on the oxygen isotopes of earlywood. Hill et al. (1995) revealed similar results for oak.

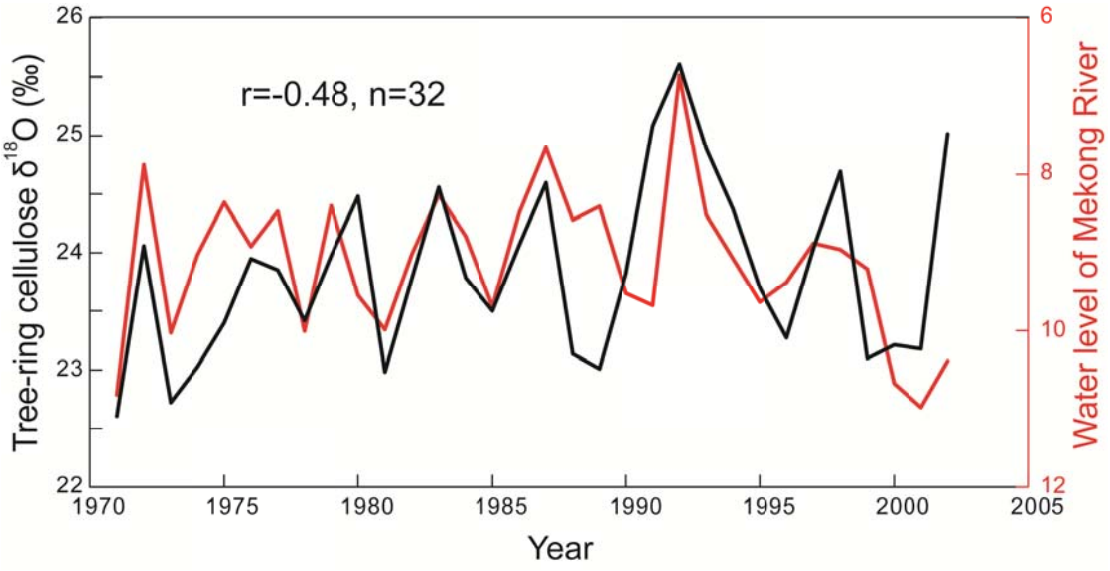

Figure 6.2 Time series of tree ring cellulose oxygen isotope in northern Laos and water level of Mekong River in Luang Probang hydrological station.

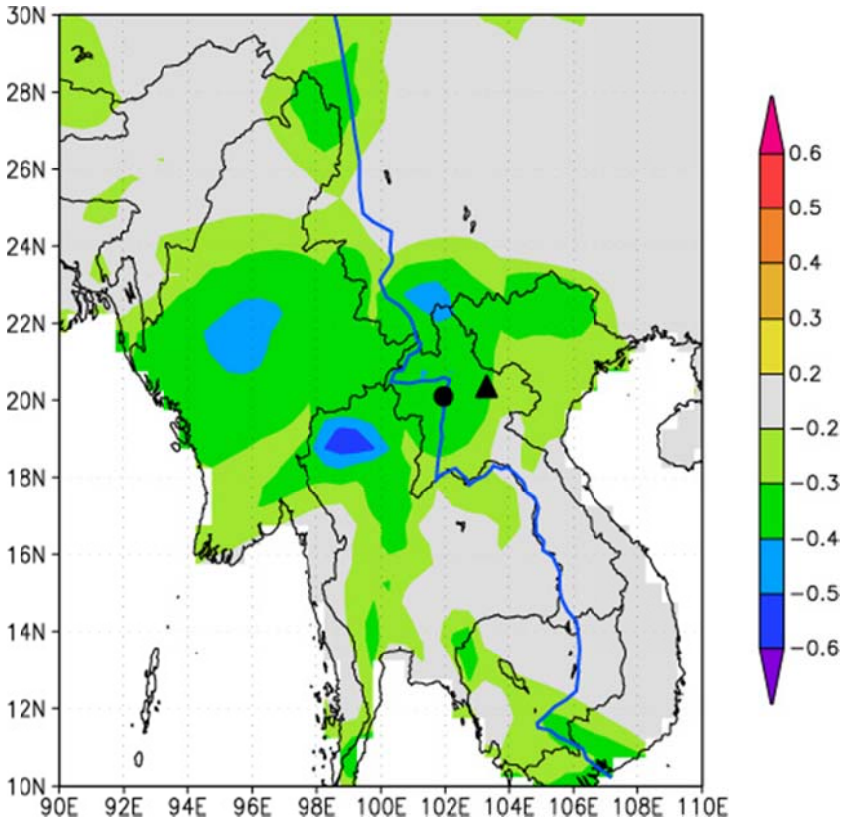

Figure 6.3 Spatial correlation between the tree ring cellulose $\delta^{18}O$ and May–October precipitation (CRU TS3.1) during 1951–2002. Black triangle shows the study area, and black circle indicates the Luang Prabang hydrological station.

In addition, there is a negative correlation ($r=-0.49$, $p<0.01$, $n=32$) between tree ring cellulose $\delta^{18}O$ and monsoon season water level of Mekong River in Luang Prabang (Figure 6.3). Spatial correlation analysis (Figure 6.3) showed that tree ring cellulose $\delta^{18}O$ has a negative correlation with monsoon season precipitation in the upper-stream area of Luang Prabang. The relationship between them provides an opportunity to reconstruct water level of Mekong River in future. Based on the correlations between PL $\delta^{18}O$ and regional climatic parameters (Figure 6.1&6.3), tree-ring cellulose $\delta^{18}O$ chronology in northern Laos can represent the regional hydroclimate in central Indo-China.

6.3 PDSI reconstructions

The mechanism that monsoon season PDSI affect tree ring cellulose $\delta^{18}O$ seems clear (Section 6.2), and monsoon season PDSI is considered to be the strongest predictor of the variance in tree-ring $\delta^{18}O$ in this area (Section 6.2). Therefore, I employ tree-ring $\delta^{18}O$ to reconstruct monsoon season PDSI using a linear regression model based on PDSI/ tree-ring $\delta^{18}O$ dataset from 1948-2002. The reconstruction model explained 41.5% of the actual PDSI variations. The fidelity of the regression model was accessed by cutting the samples into two sub-periods for calibration and verification tests (1948 to 1974 and 1975 to 2002). In order to achieve these statistical tests, the correlation coefficients (r), explained variance (r^2), reduction of error (RE), coefficient of efficiency (CE) (Cook et al., 1999) were employed. The statistical parameters (Table 6.2) show that correlation coefficient is still high during the verification period. In addition, RE and CE both were higher than zero. These test results confirmed the validity of our regression model. Besides, the reconstructed PDSI agrees well with the actual PDSI (Figure 6.4) during the overlap period (from 1948–2002). Thus, the model can be used to reconstruct monsoon season PDSI over the past 415 years.

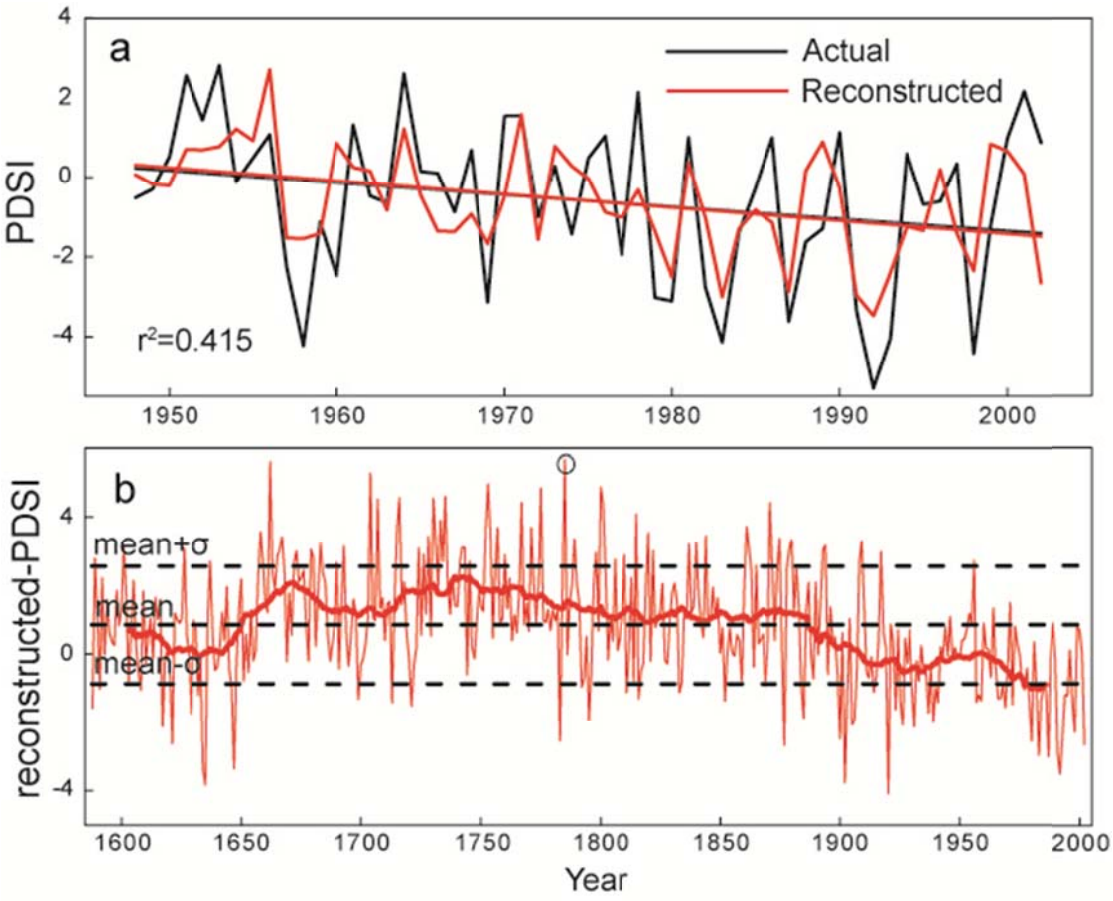

Figure 6.4. a: Actual and reconstructed PDSI values and linear regression trends, b: Reconstructions of the May–October PDSI for the period 1588–2002. The bold red line represents 31-year running average of the reconstructions.

Figure 6.4b shows the Monsoon season PDSI reconstruction from 1588-2002, and its 31-year running mean. The reconstructed PDSI values revealed that the low PDSI (dry) periods were 1630–1660, 1900-1940 and 1954-2002, and the high PDSI (wet) periods were 1660-1695, 1705-1790. Our $\delta^{18}O$-based PDSI reconstruction has a decreasing trend during the latter half of the 20th century, which parallels similar trends in meteorologically based PDSI (Figure 6.4a). In addition, Singhrattna et al. (2005) indicate that the temperature and precipitation exhibit an increasing and decreasing trend, respectively. Our monsoon season PDSI reconstruction is correlated ($r=0.73$, $p<0.001$, $n=298$) with PDSI reconstruction from Sano et al. (2012) which was

based on tree-ring $\delta^{18}O$ chronology in northern Vietnam. The reconstructed high-resolution monsoon season PDSI has the great potential to record history of drought and flood events in the past. For example, the highest PDSI value (Figure 6b, black circle) during the whole reconstructed period is 5.68 (higher than 2σ) in 1785, indicating 1785 is very wet year. According to Bangkok notable floods records from Bangkok Metropolitan Administration, a huge flood with 4.25-meter flood height happened in 1785, while flood with 1.3-meter flood height brought huge economic lost in 2011.

Table 6.2 Calibration and verification statistics for the period of 1948–2002

Calibration period	R^2	Verification period	*r*	RE	CE
Full (1948–2002)	0.415**	–	–	–	–
Early half (1948–1974)	0.298**	Late half (1975–2002)	0.652**	0.527[a]	0.399[a]
Late half (1975–2002)	0.425**	Early half (1948–1974)	0.546**	0.469[a]	0.262[a]

[a]RE, CE > 0

**$p < 0.01$

6.4 Comparison with other tree ring cellulose $\delta^{18}O$ records

In Section 6.2 & 3, I discuss that how the local climate affect tree ring cellulose $\delta^{18}O$. However, precipitation $\delta^{18}O$ which is the main controlling factor of tree ring cellulose $\delta^{18}O$ is not only affected by local climate but also influenced by atmospheric circulation (Tan et al., 2013; Vuille et al., 2005). Figure 6.5 shows the multi-year average of integrated water vapor transport during the summer (JJA), which indicates that water source of summer rainfall for southeast Asia and Himalaya is from Indian Ocean. Therefore, I investigated the relationship between tree ring cellulose $\delta^{18}O$ and main atmospheric circulation (Asian summer monsoon) that had a great influence on summer rainfall in Asia, and compared our PL $\delta^{18}O$ chronology with Asian summer monsoon Index (Webster and Yang, 1992) and three tree ring cellulose $\delta^{18}O$-based Asian summer monsoon records: 1) $\delta^{18}O$ of tree rings-an indicator of August precipitation from Reting, Tibet (Figure 6.5 & 6.6a) (Grießinger et al., 2011), 2) $\delta^{18}O$ of tree rings-an indicator of precipitation from June to September, from Hulma, Nepal Himalaya (Figure 6.5 & 6.6b) (Sano et al., 2011), 3) $\delta^{18}O$ of tree rings-an indicator of monsoon season PDSI from MCC, Northern Vietnam (Figure 6.5&6.6c) (Sano et al., 2012) in the inter-annual and multi-decadal scale.

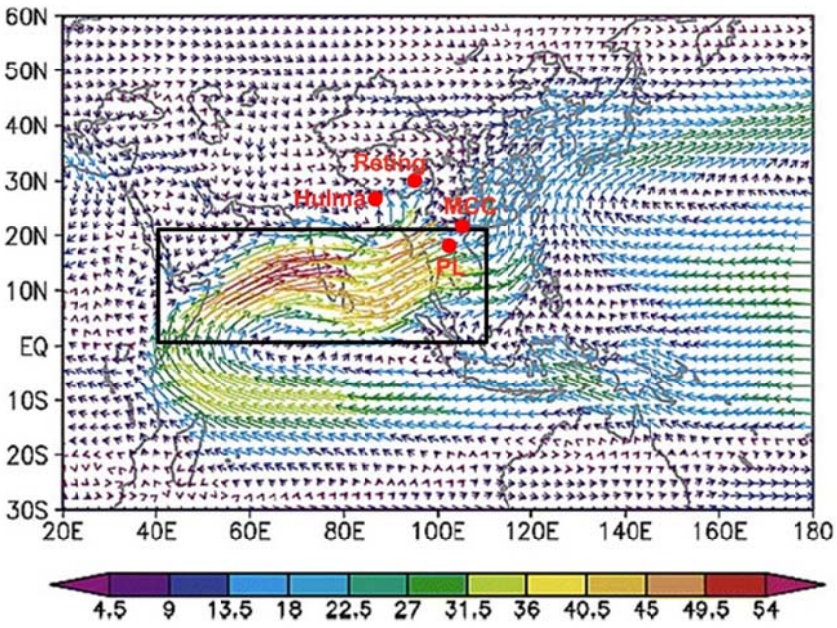

Figure 6.5 June-July-August (JJA) water vapor transport ($kg \times m^{-1}s^{-1}$). (1951–1999 average) Red spot: tree ring cellulose $\delta^{18}O$ site (PL_this sutdy, MCC, Hulma and Reting). The color of arrow shows the magnitude of the moisture flux vector. Solid box shows the region that is employed to calculate Asian summer monsoon index M (40-110E,EQ-20N). Modified from Zhou et al., 2005.

Webster and Yang (1992) provide an Asian summer monsoon index to measure the summer monsoon intensity. This monsoon index M was defined as the difference of wind velocity during summer season between the upper (u_{250}, wind anomalies in June-July-August-September at 250 hPa,) and lower (u_{850}, wind anomalies in June-July-August-September at 850 hPa,) level atmosphere (Webster and Yang, 1992):

$$M=u_{850} - u_{250}$$

At strong monsoon season, speed of wind in both the upper (250 hPa) and the lower (850 hPa) level will increase, while a reduction of wind speed at both he upper and the lower level can be observed at weak monsoon season. Hence I employed Asian monsoon Index to test the Asian summer monsoon's influences on tree ring cellulose $\delta^{18}O$ in monsoonal Asia.

The correlation between tree ring cellulose $\delta^{18}O$ in PL, MCC, Hulma and Reting with Asian Summer Monsoon Index (ASMI) is -0.48 ($n=55, p<0.01$) , -0.50 ($n=57, p<0.01$), -0.35 ($n=53, p<0.05$) and -0.19 ($n=55, p=0.167$), respectively, which indicates that tree ring cellulose $\delta^{18}O$ in PL, MCC and Hulma (Nepal) (except for Reting) is affected by Asian summer monsoon. Observed precipitation $\delta^{18}O$ data from IAEA in southeast and southwest China, Bay of Bengal show similar negative correlations with ASMI, and modeled precipitation $\delta^{18}O$ from ECHAM-4 T106 (Vuille et al., 2005) in above region is also negatively correlated with ASMI. Both observed and modeled precipitation $\delta^{18}O$ have negative correlations with ASMI in many places in monsoonal Asia, which reveal that the precipitation $\delta^{18}O$ becomes heavier at relatively strong Asian summer monsoon years, and lighter at relatively weak Asian summer monsoons years.

The mechanism underlying these correlations is that an intensified monsoon is associated with increased precipitation amount and enhanced convective activity, both of which will result in more negative precipitation $\delta^{18}O$. Because there is negative correlation between precipitation $\delta^{18}O$ and precipitation

amount (amount effect, Dansgaard, 1964). This observed ‘‘amount effect’’ is often interpreted by the condensation-related mechanism. During the condensation process, isotope-enriched water vapor is easier to be removed as condensation, leading to $\delta^{18}O$ of the remaining vapor increasingly lighter. Therefore, during the process of strong convective activity, the higher precipitation amount, the more depleted precipitation $\delta^{18}O$ (Vuille et al., 2003). However, this process cannot fully explain observed amount e□ect. Besides, several other processes can also account for the amount effect, for example, $\delta^{18}O$ of the falling rain water become less re-enriched as precipitation amount increase by either stronger exchanges with the ambient water vapor or a lower re-evaporation rate (Dansgaard, 1964). Risi et al., (2008) supported Dansgaard (1964) ideas and reproduced amount effect in marine island stations based on a single column model that includes Emanuel convective parameterization. The low correlation between tree ring cellulose $\delta^{18}O$ in Reting (Tibet Plateau) and ASMI may lie in the location of Reting which located in the north of Himalaya. Although the correlaions between tree ring cellulose $\delta^{18}O$ in Reting and ASMI for the inter-annual scales are low, tree ring cellulose $\delta^{18}O$ in Reting should be a proxy of Asian summer monsoon in long-term scales (Grießinger et al., 2011).

The mean correlation coefficient among four tree ring cellulose $\delta^{18}O$ records in Himalaya and Southeast Asia is around 0.37 for the inter-annual scale, and 0.67 for the multi-decadal scale (31-years running average) (Table 6.3). The relative high correlations in the multi-decadal scale among four tree ring $\delta^{18}O$ records reveal long–term variability of Asian summer monsoon.

Table 6.3 Correlation matrix calculated for 4 tree ring cellulose $\delta^{18}O$ time series.

r-annual	PL (this study)	MCC	Hulma
MCC	0.69 (1705-2002)		
Hulma	0.25 (1778-2000)	0.32(1778-2000)	
Reting	0.32(1588-2002)	0.24 (1705-2002)	0.38(1778-2000)

r-multi-decadal	PL (this study)	MCC	Hulma
MCC	0.67 (1620-1987)		
Hulma	0.61 (1793-1985)	0.66 ((1793-1985)	
Reting	0.79 (1602-1987)	0.60 (1720-1987)	0.71 (1793-1985)

Time period for calculating correlations was shown in the brackets.

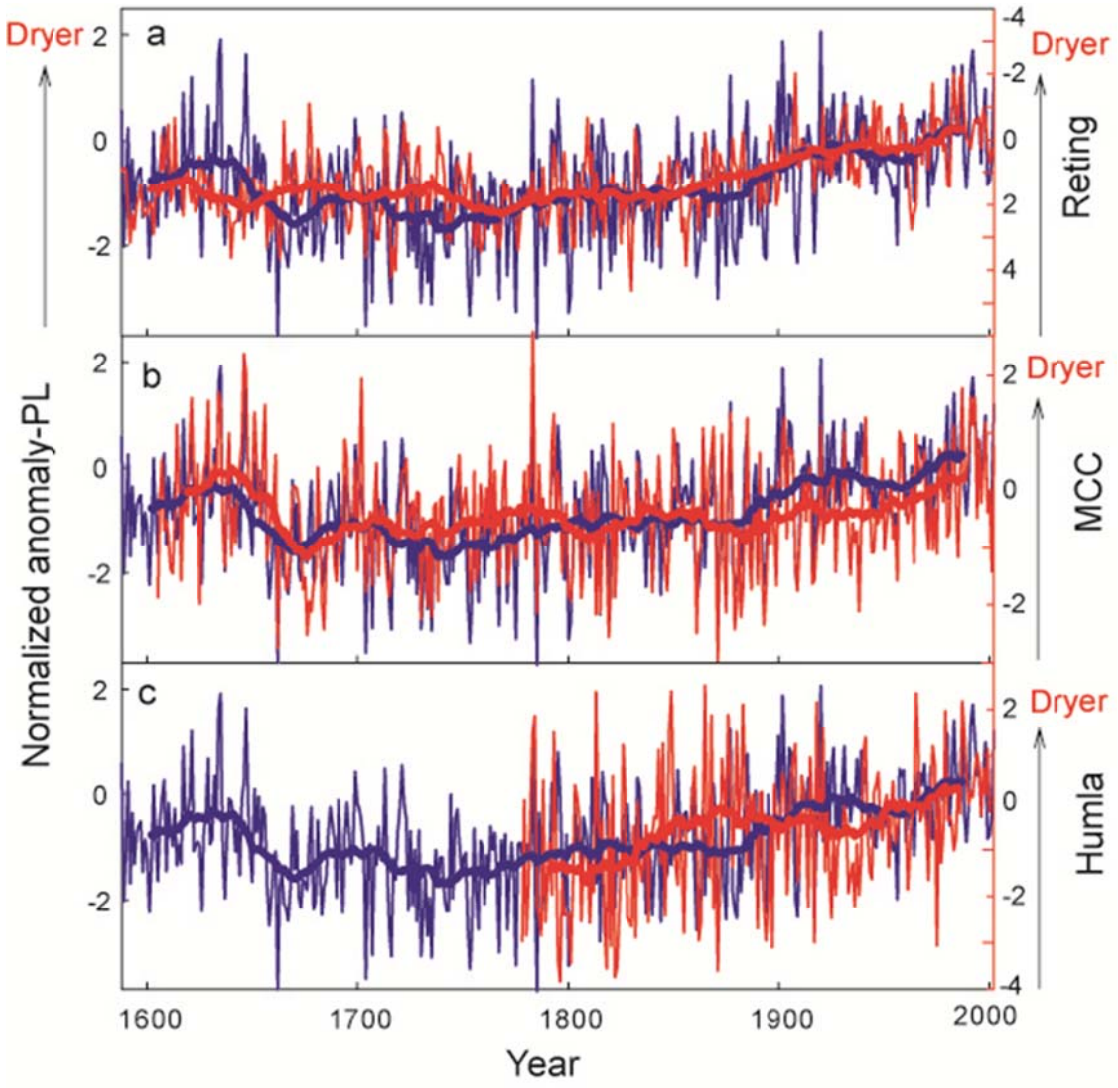

Figure 6.6 Comparison of the PL tree ring cellulose $\delta^{18}O$ series with other Asian summer monsoon records. PL tree ring cellulose $\delta^{18}O$ series (blue) along with: a, $\delta^{18}O$-based August rainfall reconstruction from Tibet (red) (Grießinger et al., 2011). b, tree ring cellulose $\delta^{18}O$ record in northern Vietnam (red) (Sano et al., 2012). c, tree ring cellulose $\delta^{18}O$ record in Nepal Himalaya (red) (Sano et al., 2011). All time series are normalized based on the period for 1951-2002 and smoothed by 31-year running average. Note that y axis of the $\delta^{18}O$-based August rainfall reconstruction from Tibet was reversed.

A noteworthy feature indicated by four tree ring cellulose $\delta^{18}O$ is decreasing Asian summer monsoon intensity during the last 200 years (Figure 6.6). In addition, lake sediment in Tibet (Chu et al., 2011) and tree ring cellulose $\delta^{18}O$ in southwest China (Xu et al., 2012) indicate that Asian summer monsoon intensity decreased since 1840 and 1860, respectively. An integrative monsoon index (IMI) (Fan et al., 2009) for south Asian summer monsoon (SASM) simulated using NCAR Climate System Model also showed a decline of SASM since 1820s. Interestingly, these consistent trends toward dry conditions are concurrent with that a consistent warming in western Indian Ocean and tropical Pacific Ocean over the last two centuries was found in coral-based SST reconstructions (Cole et al., 2000; Wilson et al., 2006) and a diatom-based SST in equatorial Pacific (Conroy et al., 2009), and thus may indicate some causal relationship between them. Considering the correlations between tree ring cellulose $\delta^{18}O$ and tropical Indian Ocean and Pacific Ocean SST (Figure 9a), increased SST over the tropical oceans may be responsible for reduction of Asian summer monsoon. Previous study show that warming in the tropical oceans leads to reduction of the Asian summer monsoon intensity, because warming in tropical oceans can weaken meridional thermal contrast between the Asian continent and adjacent oceans (Ueda et al. 2006). In addition, Fan et al. (2009) indicate that warmer sea surface temperatures in tropical Pacific are associated with a weakened SASM.

7 The relationship between ENSO and tree ring cellulose $\delta^{18}O$ in Southeast Asia

7.1 The linkage between ENSO and tree ring cellulose $\delta^{18}O$ in Southeast Asia

ENSO, which is often linked with extreme weather events such as flooding and drought has an important effect on climate and society in Asian monsoon areas (Diaz and Markgraf, 2000). Many previous reports (Buckley et al., 2005, 2007a; Sano et al., 2009) have investigated the relationship between the climate in Southeast Asia and ENSO using TRWi. Moreover, TRWi has been used in the southwestern United States to reconstruct the history of ENSO (Li et al., 2011a; Mann et al., 2000). However, tree-ring cellulose $\delta^{18}O$ usually displays higher signal strengths than TRWi. Based on our results, the $\delta^{18}O$ chronology shows a close link with April-October Nino 3.4 SST (Figure 7.1a) and has similar variations with MEI during the last fifty years. In addition, the $\delta^{18}O$ chronology shows peak values in 1958, 1965, 1969, 1972, 1983, 1987, 1992, 1998 and 2002, when El Niño events happened in the previous winter and/or current summer. Lower values of tree-ring cellulose $\delta^{18}O$ emerge in 1956, 1964, 1971, 1989, 1999 and 2000, when La Niña events occurred in the prior winter and/or current summer. Our results appear to show links between tree-ring cellulose $\delta^{18}O$ in Laos and ENSO, and they indicate that the tree-ring cellulose $\delta^{18}O$ in Laos may be a promising proxy to record ENSO. Previous studies in Indonesia (Poussart et al., 2004) and Peru (Evans and Schrag, 2004) showed that intra-annual tree-ring cellulose $\delta^{18}O$ time series had the potential

to record El Niño. Compared with previous studies (Evans and Schrag, 2004, Poussart et al., 2004), our $\delta^{18}O$ chronology can reflect El Niño using less samples.

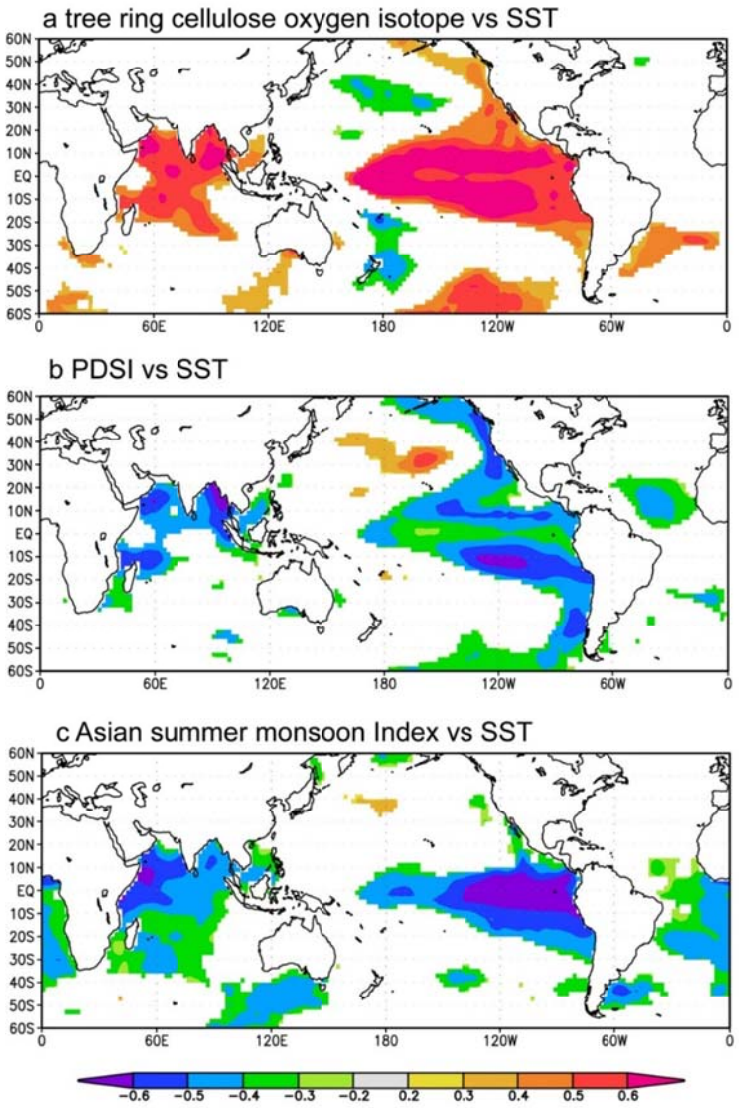

Figure 7.1 Spatial correlations between PL $\delta^{18}O$ record (a)/May-October PDSI(b)/Asian summer monsoon index (c) and April-October sea surface temperatures (NCDC v3 data set) for the period 1951–2002. Correlations that are not significant at the 95% level have been masked out.

I can infer that the following factors cause the link between tree-ring cellulose $\delta^{18}O$ in northern Laos and ENSO. First, an El Niño/La Niña event that happen in tropical Pacific can result in drought/wet conditions over Indochina (Meehl and Hu, 2006). This relationship was proved by the spatial correlations between PDSI and sea surface temperatures (NCDC v3 data set) in the period of 1951–2002 with meteorological data (Figure 7.1b) and in the period of 1856-2006 by reconstructed PDSI (Buckley et al., 2010). PDSI strongly affect changes of tree ring cellulose $\delta^{18}O$ by relative humidity (detailed discussion in Section 6.2). Therefore, El Niño-like (warm-phase) configuration result in drought (negative values of the PDSI) in Southeast Asia, which lead to enriched tree ring cellulose $\delta^{18}O$ by enhanced evapotranspiration.

Second, rainfall of Asian summer monsoon rainfall would decrease in an El Nino developing year (Webster et al., 1998), which was supported by spatial correlations between Asian summer monsoon precipitation and SST (NCDC v3 data set) in the period of 1951–2002. Besides, El Niño results in a reduction of summer monsoon rainfall in Southeast Asia (Chen and Yoon, 2000; Singhrattna et al., 2005). It needs to be emphasized that, in the base map in Figure 6.5 which shows the multi-year average of integrated water vapor transport, there appears to be no influence of the Pacific atmospheric circulation on the Southeast Asia but this is misleading. In general, the water vapor source of precipitation in May-June-July (MJJ) is from the Bay of Bengal, Indian Ocean, while the moisture of rainfall in September-October (SO) originate from the South China Sea. In detail, East Asian summer monsoon (EASM), western north Pacific summer monsoon (WNPSM) and Indian summer monsoon (ISM) control the monsoon season climate in northern Southeast Asia (Wang and LinHo, 2002). The EASM and WNPSM would be more influenced in the year after the El Nino mature phase (Wang et al., 2003). Specifically, subsidence has significant effects on the Philippine Sea and

Southeast Asia, resulting in deficient WNP monsoon rainfall (Wang et al., 2000) during the year after the El Nino mature phase. For example, El Nino conditions were developing in the tropical Pacific in the fall of 1997, rainfall in South China Sea was reduced by 37% in June-July-August of 1998 (Wang et al., 2003). Normalize $\delta^{18}O$ value of PL chronology is 1.32 (higher than 1σ), which indicate the dryer condition of monsoon season in 1998. Therefore, either ISM or WNPSM was reduced/enhanced by El nino/La nina, ENSO events can be recognized by tree ring cellulose $\delta^{18}O$ through two summer monsoon system, which strengthen tree ring cellulose $\delta^{18}O$ ability to record the ENSO events.

7.2 MEI Reconstruction and comparison with other ENSO Reconstructions

Anomalous precipitation (drought and flood) events associated with ENSO are the natural disasters that have great influences on people in Southeast Asia. Our $\delta^{18}O$ chronology as a predictor of PDSI should be used as a proxy of ENSO due to the great influences of ENSO on PDSI in Southeast Asia (Buckley et al., 2010). Previous studies (Sano et al., 2012; Xu et al., 2011) show that tree ring $\delta^{18}O$ in Laos and Vietnam has closed relationship with ENSO. In this part, three longest cores (PL101a, PL126a, PL136b) from PL site in Laos and two longest cores (MCC2, MCC6) from MCC site in Vietnam

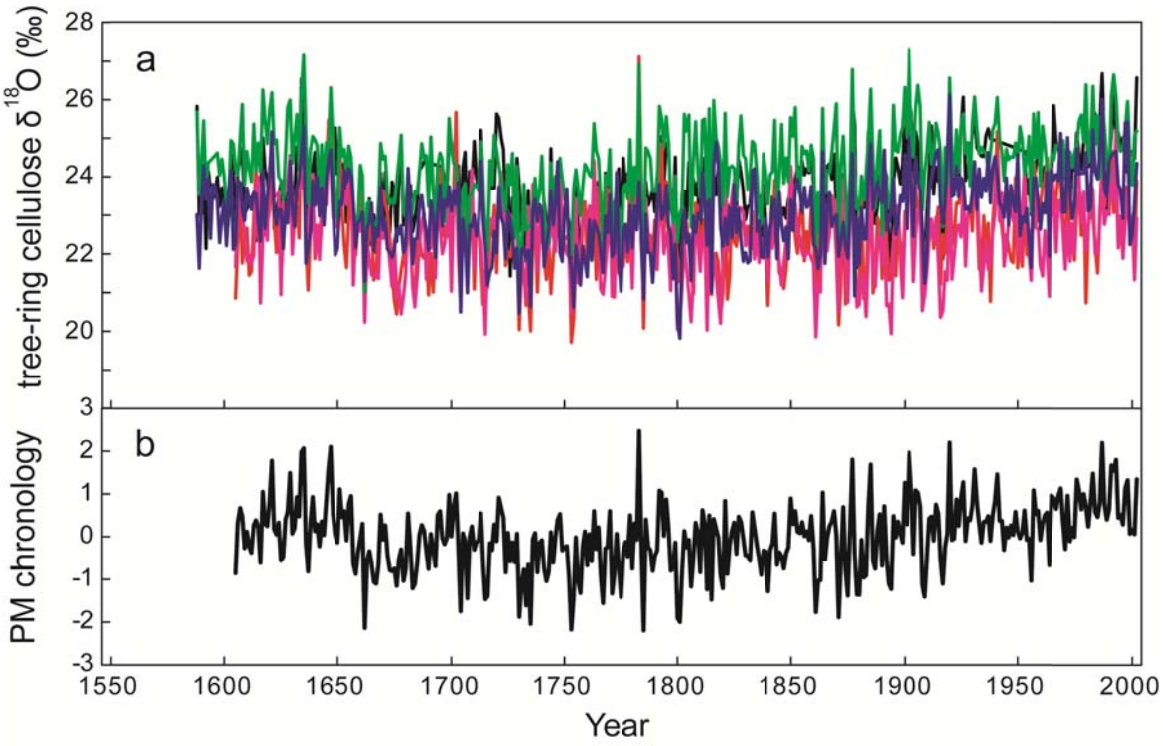

Figure 7.2 a; Tree ring cellulose $\delta^{18}O$ time series from PL site (PL101a, PL126a, PL136b) and MCC site (MCC02, MCC06). b; The composite chronology from five samples

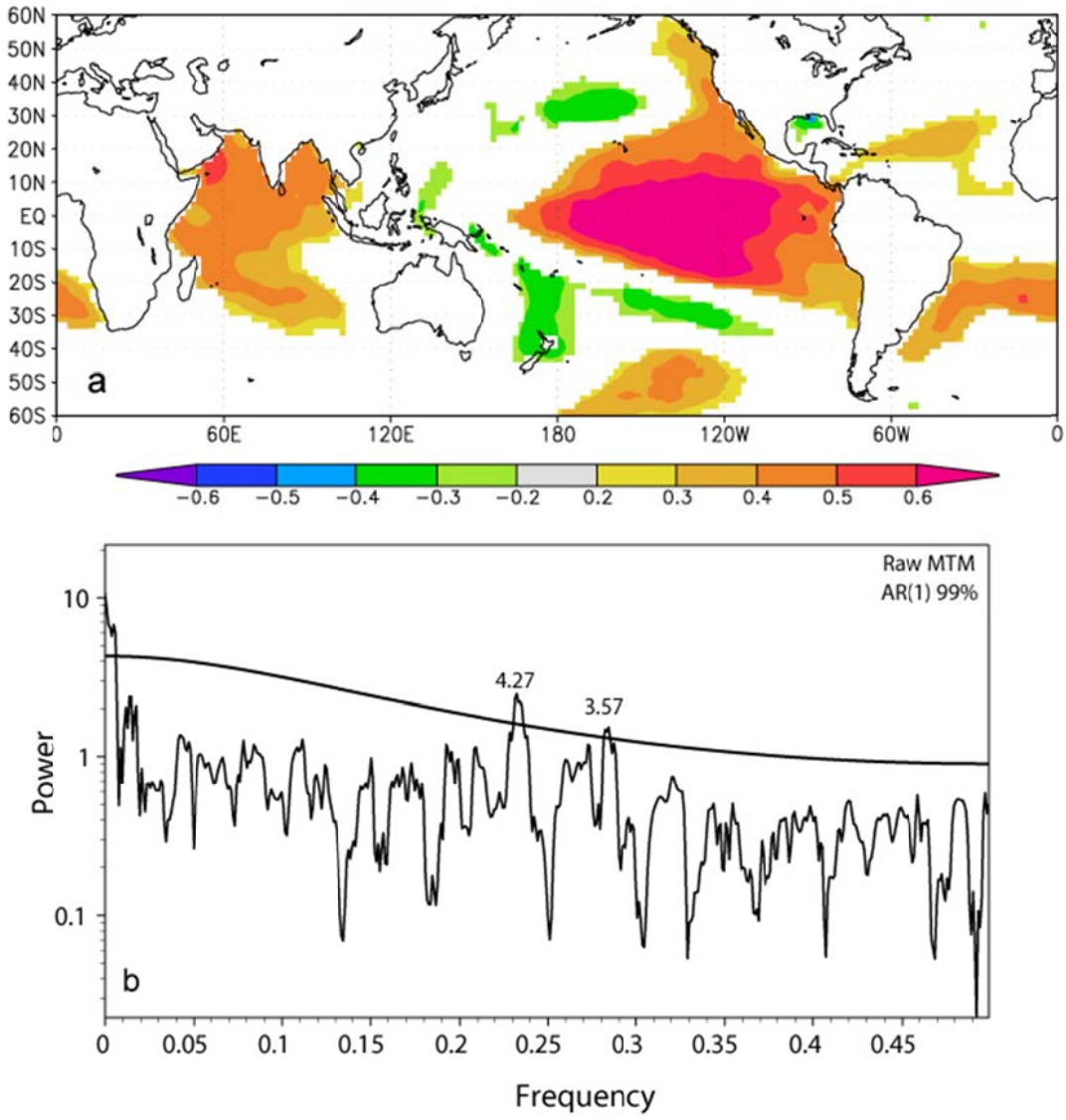

Figure 7.3. a: Spatial correlations between PM δ18O record and annual (prior-year November to current-year October) sea surface temperatures (NCDC v3 data set) for the period 1872–2002, b; Multitaper method power spectra for the PM $\delta^{18}O$ record (AD 1605–2002). Peaks above the solid line are significant at the 99% level of confidence.

were selected with 398-year common period (1605-2002) to extract the local ENSO signal. These five cores (Figure 7.2a, PL101a, PL126a, PL136b, MCC2, MCC6) from two sites show high correlations (0.58, 0.59, 0.59, 0.57, 0.54) with MEI. Due to differences in the absolute $\delta^{18}O$ values between cores, five oxygen isotope time series were individually normalized over the entire time period based on the common period 1605–2002. the z-scores are calculated from $Z_t = (x_t – m_x)/s_x$, where x_t represents the values of $\delta^{18}O$ in year t, and m_x and s_x are the average of the mean and standard variation, respectively, of the other five cores between 1605 and 2002. The five series were then averaged to produce the final $\delta^{18}O$ chronology for the period 1605–2002 (Figure 7.2b). The composite chronology is called PM $\delta^{18}O$ chronology, which is significantly correlated with ENSO-related indices during the 1872–2002 period, especially annual (from previous November to current October) SOI ($r = –0.53$, $p < 0.001$, $n=121$), Nino 3.4 SST ($r = 0.66$, $p < 0.001$, $n=131$), and the MEI ($r = 0.71$, $p < 0.001$, $n=131$) (Figure 7.4a).

Besides, spatial correlation analysis between PM chronology and SST (Figure 7.3a) show ENSO's significant influences on PM chronology, and spectral power analysis (Figure 7.3b) by multi-taper method (Mann and Lees, 1996) indicates that significant peaks of PM $\delta^{18}O$ chronology are found at 3.57 and 4.27 years that fall within the range (2-7 years) of ENSO variability. Comparison between ENSO events record and higher/lower value of tree ring cellulose $\delta^{18}O$ in last 131 years indicate that El Niño and La Niña phases result in dry and wet conditions, respectively, in the study region.

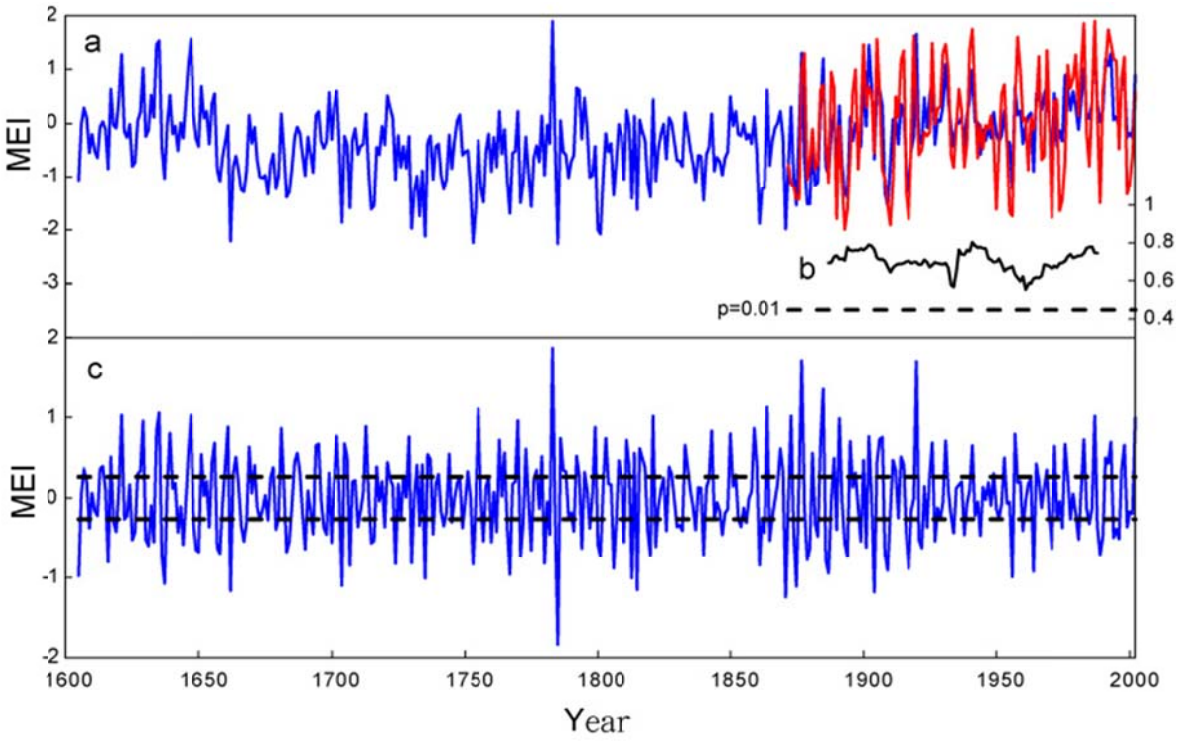

Figure 7.4. a: Reconstructed and observed annual (prior-year November to current-year October) MEI Time series, b: running 31-year correlations between data sets, c: high frequency signal (<9 years) of reconstructed annual MEI, dash lines means 0.5 standard deviation.

Table 7.1 Correlation Matrix Calculated for 7 ENSO Reconstructions From the 1871–1980 and 1605–1870 Periods

	Source proxy location	Reference	This study	Wilson COA	Wilson TEL	Cook	Mann	Li
1871–1980								
	Central/Eastern Pacific	Wilson[b] (COA,CPR)	0.55					
	Indo-Pacific Basin[a]	Wilson[b] (TEL,CPR)	0.68	0.8				
	Southwest N America	Cook[c]	0.44	0.6	0.48			
	Near Global	Mann[d]	0.46	0.64	0.53	0.82		
	North America	Li[e]	0.37	0.34	0.28	0.69	0.67	
	Pacific Basin	Braganza[f]	0.48	0.55	0.54	0.71	0.72	0.6
		McGregor[g]	0.47					
1605–1870								
		Wilson[b] (COA)	0.09 [ns]					
		Wilson[b] (TEL)	0.23	0.03 [ns]				
		Cook[c]	0.25	0.00 [ns]	0.16 [ns]			
		Mann[d]	0.28	0.15 [ns]	0.14 [ns]	0.48		
		Li[e]	0.17 [ns]	-0.06 [ns]	0.06 [ns]	0.61	0.39	
		Braganza[f] (R5)	0.29	-0.02 [ns]	0.22	0.66	0.59	0.48
		McGregor[g]	0.32					

a:Superscript ns denotes non-significant ($p > 0.05$). b:Wilson et al.(2010); c:Cook et al. (2008); d:Mann et al. (2000). e: Li et al.(2011); f:Braganza et al.(2009); g: McGregor(2010)

The proportion of instrumental variances for annual MEI (1872-2002) explained by PM $\delta^{18}O$ chronology are 50%, which has better performances than previous efforts (Mann et al. 2000; Braganza et al 2009) at ENSO-related index reconstruction. In detail, Mann et al. (2000) resolved 34–42% of instrumental Nino 3 SST (October to March) by three Empirical Orthogonal Function (EOFs), and Braganza et al (2009) account for 48% of Nino 3.4 SST using ENSO sensitive proxies from Pacific basin. It should be noted that Mann et al. (2000) and Braganza et al (2009) employed many proxies including tree ring width chronologies from southwest America and New Zealand, ice core and coral records, while I just used two tree ring cellulose $\delta^{18}O$ chronologies. Our results indicate tree-ring $\delta^{18}O$ from Indo-China has significant potential to produce independent and robust reconstructions of ENSO variability to explore the spatial influence of ENSO events in the past.

However, ENSO-monsoon relationships are characterized by nonstationarity process. For example, an inverse relationship between ENSO and the Indian summer monsoon has broken down since the 1980s (Kumar et al., 1999). Recent research by Singhrattna et al. (2005) reveals an increase in the influence of ENSO over central Thailand since the 1980s.

The relationship between local climate and the eastern equatorial Pacific SST was also found in the tree ring cellulose $\delta^{18}O$-based local climate and ENSO index (Liu et al., 2011; Sano et al., 2012; Sano et al., 2011; Xu et al., 2011). For example, the PDSI reconstructed from tree ring cellulose $\delta^{18}O$ in the Nepal Himalaya shows a negative correlation with the June–September eastern equatorial Pacific SST (Sano et al., 2011). However, the tree ring cellulose $\delta^{18}O$-ENSO relationship is not stable. For example, tree ring cellulose $\delta^{18}O$ in Yunnan, southwest China and the Amazon lost correlations with the SOI and NINO 3.4 SST during the periods 1930–1980 and 1925–1975, respectively (Brienen et al., 2012; Liu et al., 2011). Besides, tree ring cellulose $\delta^{18}O$ in Fujian, southeast China (Xu et al., submitted) also shows a close link with March–October eastern equatorial Pacific SST during the period from

1890-2010, except for the period between 1920 and 1960.

There was lower ENSO variance (Mason, 2001; Torrence and Webster, 1999) between 1920 and 1960. These results indicate that the reduced ENSO variance may lead to a subsequently reduced influence on remote areas as the teleconnection becomes unstable.

Nevertheless, correlation between PM $\delta^{18}O$ chronology and ENSO are time-stable (Figure 7.4b). Our results imply that northern Indochina may be a 'hot spot' firmly teleconnected with the tropical Pacific. The significant time-stable correlation between tree our overall results indicate the significant potential for generating independent and robust reconstructions of ENSO variability using tree ring $\delta^{18}O$ from mainland Southeast Asia, and for investigating the geographical influence of ENSO before the instrumental period.

Our MEI reconstruction can pass rigorous statistical tests (RE, CE data not shown) and correlation between PM $\delta^{18}O$ chronology and ENSO are time-stable (Figure 7.4b). Through the comparison between our MEI reconstruction with other ENSO reconstructions (Braganza et al., 2009; Cook et al., 2008; Li et al., 2011; Mann et al., 2000; McGregor, 2010; Wilson et al., 2010), I found that existing ENSO are in good agreement for the period since 1871 (the time at which instrumental records commenced), there is relatively limited agreement about ENSO variability prior to this time (Wilson et al., 2010). As presented in Table 7.1, our reconstructed MEIs also show markedly weakened associations with published ENSO reconstructions before the instrumental period. Among the ENSO reconstructions, the 'center of action' (COA) reconstruction (Wilson et al., 2010) is perhaps the most reliable, as its calibration model accounts for over 80% of the instrumental variance. The importance of the COA reconstruction is further emphasized by the fact that all of the original proxy (coral) records are located in the central and eastern Pacific (the core region where ENSO develops), while other reconstructions rely largely on proxy records located in regions that are teleconnected with the

central Pacific. Unfortunately, the COA reconstruction is not considered robust prior to 1850, because of lack of replication (Wilson et al., 2010); this lack of sample replication may be responsible for reduced inter-series correlations before the mid-19th century. It should be noted that the ENSO reconstructions of Mann et al. (2000), Cook et al. (2008), Braganza et al.(2009), and Li et al. (2011) are in moderate agreement prior to 1871. This is due partly to the shared tree ring data from southwest North America for these reconstructions. The cross correlations, however, do indicate some degree of coherence among these reconstructions. On the other hand, the 'teleconnection' (TEL) reconstruction, based on 1 ice core and 11 coral records from the Indo-Pacific basin (but out of the region used for the COA reconstruction) (Wilson et al., 2010), is less well correlated with those reconstructions (Braganza et al., 2009; Cook et al., 2008; Li et al., 2011; Mann et al., 2000) for the period 1705 – 1870, although the TEL record is considered as robust since 1727. These results, taken together with the fact that the TEL series is entirely independent of the reconstructions produced by Cook et al. (2008) and Li et al. (2011), indicate that the teleconnected relationship between the tropical central/eastern Pacific and the regions where proxy records are located may not be temporally stable (Wilson et al., 2010). So I should be very cautious about whether the reconstructed MEI reflect true ENSO situation in centre of action (COA) beyond the calibration period (1872-2002). Therefore, it is safer to consider our MEI reconstruction as local ENSO record.

7.3 Local ENSO events history in Southeast Asia

To capture discrete El Nino and La Nina events, high-frequency signal (less than 9 years) of reconstructed MEI are preserved (Figure 7.4b), and 0.5 standard deviations as a threshold level for ENSO events of was chose, which is same criterion that was used for defining the El Niño and La Niña events.(McGregor 2010). Looking at the correspondence between the PM and observations during 1951-2002, I find that: reconstructed local El nino events are in 1953, 1957, 1965, 1969, 1972, 1983, 1987, 1991, 1992, 1993, 1997, 1998, and 2002, when El Niño events (observations) happened in the previous winter and/or the current summer (except 1993), while reconstructed local La Niña events emerge in 1956, 1960, 1964, 1971, 1973, 1975,1978,1981,1985, 1988, 1989, 1994, 1995, 1996 and 1999 (except 1960, 1978, 1981), when La Niña events occurred in the prior winter and/or the current summer.

I continue the evaluation of the fidelity of the PM $\delta^{18}O$ chronology to capture discrete El Nino and La Nina events against chronologies of El Nino based on multi-proxy reconstruction (Gergis and Fowler, 2009) and historical records (Ortlieb, 2000; Quinn, 1993) and La Nina events (Gergis and Fowler, 2009). Based on previous discussion on how ENSO events affect local climate in Southeast Asia, I make the assumption that the reconstructed ENSO events by PM $\delta^{18}O$ record fell in the global ENSO events reconstruction (Gergis and Fowler, 2009) in the year of the event or the year following. 121 El Nino events identified by PM $\delta^{18}O$ record between 1605–2002 (Table 7.2), approximately 50.94%, 58.68%, 68.22% are registered in Ortileb (2000), Gergis and Fowler (2009) and Quinn (1993), and 130 La Nina events were identified in the PM $\delta^{18}O$ record, 82.46% are registered in global ENSO events reconstruction (Gergis and Fowler, 2009) (Table 7.3).

Table 7.2 El Niño events detected by the PM-based reconstruction MEI with classified El Niño events from events form Gergis and Fowler (2009)

El Niño Year	reconstructed MEI	El Niño events Gergis and Fowler (2009)	El Niño Year	reconstructed MEI	El Niño events Gergis and Fowler (2009)
1607	0.358	1607(VS)	1808	0.457	1807(S)
1613	0.357	1614(W)	1809	0.266	/
1614	0.387	1614(W)	1811	0.711	1812(S)
1617	0.505	1618(VS)	1812	0.400	1812(S)
1621	1.026	1621(W)	1814	0.549	1814(W)
1627	0.304	/	1816	0.608	1815(W); 1816(W)
1628	0.331	/	1817	0.486	1816(W);
1629	0.952	/	1818	0.369	1817(S)
1634	0.838	1635(M)	1821	1.014	/
1635	1.055	1635(M)	1827	0.379	/
1639	0.801	1639(W)	1828	0.299	1829(W)
1646	0.561	1646(W)	1833	0.650	1832(W);1833(S)
1647	1.025	1646(W); 1648(M)	1834	0.378	1833(S)
1651	0.534	1650(E); 1651(W)	1843	0.828	1844(M)
1655	0.435	/	1850	0.793	/
1656	0.677	/	1852	0.287	1852(W)
1660	0.391	1659(M);1660(VS)	1859	0.861	1858(M)
1661	0.877	1661(S)	1860	0.405	1860(W)
1663	0.297	/	1864	1.124	1864(W)
1664	0.501	1665(W)	1869	0.605	1868(VS)
1669	0.629	1669(W)	1870	0.318	/
1671	0.398	/	1873	1.012	1874(W)
1678	0.371	/	1876	0.269	1876(W)
1681	0.860	/	1877	1.713	1877(VS)
1686	0.438	1687(VS)	1881	0.550	1881(M)
1687	0.551	1687(VS)	1884	0.671	1884(W)
1688	0.314	1687(VS)	1885	1.352	1885(S)
1694	0.643	1694(S)	1889	0.486	1889(W)
1695	0.665	1695(W)	1891	0.982	1891(VS)
1699	0.310	1700(W)	1895	0.698	1896(M)
1702	0.764	/	1897	0.314	1897(S)
1705	0.668	/	1900	0.463	1900(VS)
1706	0.502	1707(W)	1902	0.759	1902(VS)
1713	0.884	1712(W);1713(M)	1905	0.433	1905(E)
1717	0.381	1718(E)	1906	0.725	1906(W)
1721	0.434	1720(W);1721(W)	1907	0.748	1906(W)

E: Extreme; VS: Very Strong; S: Strong; M: Moderate; W: Weak from Gergis and Fowler (2009)

Table 7.2 El Niño events detected by the PM-based reconstruction MEI with classified El Niño events from events form Gergis and Fowler (2009) (Continued)

El Niño Year	reconstructed MEI	El Niño events Gergis and Fowler (2009)	El Niño Year	reconstructed MEI	El Niño events Gergis and Fowler (2009)
1727	0.278	1726(W)	1911	0.461	1911(M)
1729	0.755	1728(S); 1729(W)	1912	0.341	1912(VS)
1732	0.403	/	1914	0.504	1914(VS)
1734	0.407	1734(W)	1915	0.409	1915(VS)
1736	0.534	1737(E)	1920	1.703	1920(W)
1737	0.472	1737(E)	1925	0.280	1924(W);1925(S)
1740	0.296	/	1926	0.679	1926(E)
1744	0.539	1744(W)	1931	0.704	1931(S)
1751	0.329	/	1941	0.645	1940(VS);1941(E)
1755	1.103	1754(W)	1949	0.304	1949(W)
1763	0.715	/	1953	0.492	1952(W)
1765	0.554	1766(W)	1957	0.789	1957(S)
1770	0.958	1770(VS)	1965	0.415	1965(S)
1773	0.601	/	1969	0.348	1969(S)
1777	0.345	1777(W)	1972	0.636	1972(M)
1779	0.509	/	1976	0.660	1976(M)
1783	1.870	1782(W); 1783(M)	1983	0.719	1983(E)
1786	0.737	/	1987	1.013	1987(VS)
1787	0.347	/	1991	0.490	1991(VS)
1788	0.329	/	1992	0.424	1992(VS)
1792	0.514	1791(VS);1792(W)	1993	0.690	1992(VS)
1793	0.279	1792(W);1793(M)	1997	0.352	1997(W)
1795	0.321	1794(M)	1998	0.650	1997(W)
1799	0.874	1798(W); 1799(S)	2002	0.989	2002(E)
1803	0.738	1803(S)			

E: Extreme; VS: Very Strong; S: Strong; M: Moderate; W: Weak from Gergis and Fowler (2009)

Table 7.3 La Niña events detected by the PM-based reconstruction MEI with classified La Niña events from events form Gergis and Fowler (2009)

La Niña Year	reconstructed MEI	La Niña events Gergis and Fowler (2009)	La Niña Year	reconstructed MEI	La Niña events Gergis and Fowler (2009)
1605	-0.977	1605(M)	1800	-0.585	1801(VS)
1609	-0.376	/	1801	-0.727	1801(VS)
1616	-0.800	/	1806	-0.880	1805(VS)
1618	-0.299	/	1807	-0.275	1808(VS)
1619	-0.420	/	1810	-0.551	1810(S)
1622	-0.264	1622(S)	1813	-1.003	1813(M)
1625	-0.522	1625(M)	1815	-1.153	/
1626	-0.423	1626(VS)	1819	-0.402	1819(S)
1630	-0.521	1630(S)	1820	-0.718	1820(S)
1631	-0.597	1631(VS)	1822	-0.609	1823(M)
1633	-0.549	1632(VS)	1826	-0.407	1825(M)
1636	-0.722	1635(W)	1830	-0.358	/
1637	-1.072	1637(S)	1831	-0.337	/
1642	-0.427	1642(S)	1832	-0.408	/
1644	-0.584	1644(S)	1837	-0.398	/
1648	-0.316	1648(W)	1840	-0.709	1840(W)
1649	-0.646	1649(W)	1844	-0.272	1843(W)
1650	-0.678	1649(W)	1847	-0.458	1847(S)
1654	-0.363	1654(VS)	1854	-0.357	/
1657	-0.622	1658(M)	1856	-0.306	/
1658	-0.694	1658(M)	1861	-0.843	1860(VS)
1662	-1.165	1663(VS)	1863	-0.436	1863(VS)
1666	-0.340	/	1865	-0.530	1864(W)
1667	-0.540	1668(M)	1871	-1.243	1871(VS)
1668	-0.298	1668(M)	1874	-0.438	1874(S)
1673	-0.273	/	1875	-1.108	1875(S)
1676	-0.276	1676(S)	1879	-0.774	1879(E)
1679	-0.392	1678(M)	1880	-0.634	1880(VS)
1683	-0.674	/	1882	-0.323	/
1684	-0.545	1685(S)	1883	-0.478	/
1690	-0.639	1690(M)	1886	-0.780	1886(M)
1693	-0.448	/	1887	-0.943	1887(VS)
1697	-0.374	1696(VS)	1890	-0.395	1890(S)
1698	-0.455	/	1893	-0.563	1893(VS)
1700	-0.555	1701(M)	1894	-0.730	1894(E)

E: Extreme; VS: Very Strong; S: Strong; M: Moderate; W: Weak from Gergis and Fowler (2009)

Table 7.3 La Niña events detected by the PM-based reconstruction MEI with classified La Niña events from events form Gergis and Fowler (2009) (Continued)

La Niña Year	reconstructed MEI	La Niña events Gergis and Fowler (2009)	La Niña Year	reconstructed MEI	La Niña events Gergis and Fowler (2009)
1704	-1.099	/	1899	-0.540	/
1707	-0.848	1708(M)	1901	-0.615	/
1710	-0.360	1709(M)	1904	-1.179	1904(W)
1715	-0.563	1715(S)	1908	-0.696	1907(M)
1716	-0.535	1716(S)	1909	-0.906	1909(VS)
1720	-0.362	/	1916	-0.443	1916(S)
1724	-0.824	1724(M)	1917	-0.886	1917(VS)
1730	-0.816	1730(W)	1921	-0.521	1921(W)
1733	-0.342	1733(VS)	1922	-0.624	1922(S)
1735	-1.008	1735(W)	1924	-0.366	1923(W)
1738	-0.451	1739(VS)	1927	-0.538	/
1742	-0.347	1742(E)	1934	-0.434	1934(W)
1745	-0.300	1745(S)	1938	-0.458	/
1749	-0.371	1748(W)	1944	-0.467	1943(W)
1753	-0.829	1753(S)	1956	-0.990	1956(VS)
1757	-0.537	1757(M)	1960	-0.407	1960(W)
1760	-0.552	1761(M)	1964	-0.919	1963(W)
1762	-0.421	1761(M)	1971	-0.628	1971(VS)
1766	-0.366	1765(S)	1973	-0.274	1973(W)
1767	-0.959	/	1975	-0.371	1975(S)
1771	-0.731	1772(M)	1978	-0.264	/
1772	-0.304	1772(M)	1981	-0.516	/
1775	-0.653	1776(W)	1985	-0.320	1985(W)
1780	-0.819	1780(S)	1988	-0.356	1988(M)
1782	-0.455	1782(W)	1989	-0.706	1989(VS)
1784	-0.278	1785(W)	1990	-0.488	1990(VS)
1785	-1.840	1785(W)	1994	-0.494	1995(S)
1791	-0.414	1790(S)	1995	-0.384	1995(S)
1794	-0.628	1795(W)	1996	-0.511	1996(M)
1797	-0.377	1797(M)	1999	-0.361	1998(E)

E: Extreme; VS: Very Strong; S: Strong; M: Moderate; W: Weak from Gergis and Fowler (2009)

The total number of corresponding El Nino events that were identified by the PM $\delta^{18}O$ record and Ortileb (2000) El Nino chronology is smaller than two other El Nino chronologies. El nino event chronology of Ortileb (2000) was just based on documentary records in Peru, while the El Nino chronology of Gergis and Fowler (2009) was derived from tree ring, coral, ice and documentary records from Pacific basin, North Asia and North African and El Nino chronology of Quinn (1993) that included India, Eastern Hemisphere and Chile-Peru data was considered as global ENSO chronology. The PM $\delta^{18}O$ record hit more La nina events than El Nino events of Gergis and Fowler (2009), which may indicate that spatial teleconnection pattern of El Nino and La Nina have some discrepancies. However, more paleo-La Nina records are needed for further investigations. Nevertheless, our results provide independent local ENSO history, which is helpful for investigating the geographical influence of ENSO before the instrumental period.

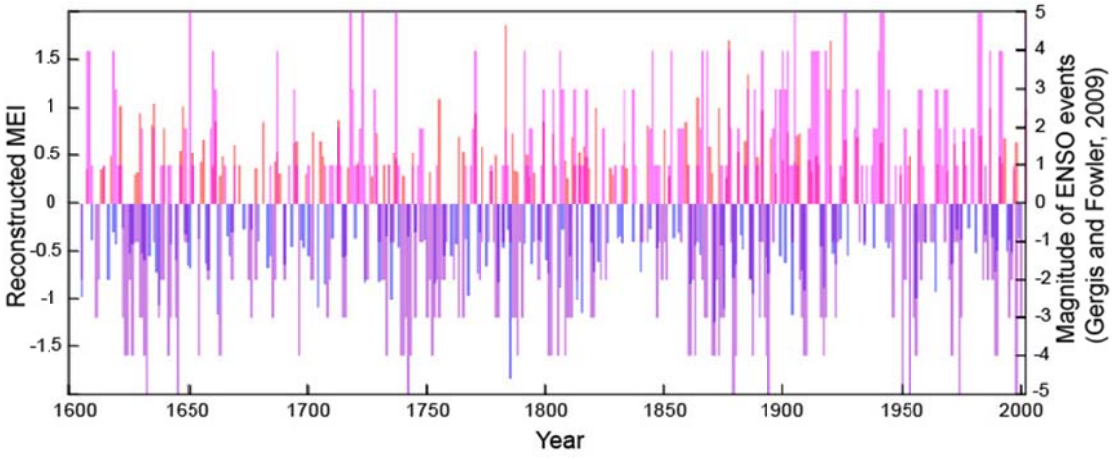

Figure 7.5 Comparison between reconstructions of local El Nino (red)/La Nina (blue) events and global El Nino (pink)/La Nina (purple) events (Gergis and Fowler, 2009). Magnitude of ENSO events: 5(-5)-extreme; 4(-4)-very strong; 3(-3)-strong; 2(-2)-moderate; 1(-1)-weak for El Nino (La Nina) events.

Conclusion

By analyzing the intra-annual tree ring cellulose $\delta^{18}O$ for trees without distinct rings (*Styrax* and *Ficus sp*) in northern Laos and measuring seven cores of *Fokienia hodginsii* with annual-resolution in natural forest in northern Laos during the period of 1588-2002, I provide evidence that tree ring cellulose $\delta^{18}O$ in northern Laos has great potential for paleoclimate research. The main findings of this study are as follows:

1) High-resolution cellulose $\delta^{18}O$ of *Styrax* and *Ficus sp* showed clear annual cycles with amplitude, which is also supported by modeled tree ring cellulose $\delta^{18}O$ based on tree ring cellulose $\delta^{18}O$ fractionation model and climate data near the study area. These annual cycles of tree ring cellulose $\delta^{18}O$ provide a new method to measure annual growth for tropical trees without distinct annual rings.

2) Compared with tree ring width, tree ring cellulose $\delta^{18}O$ show more consistent variations between different trees, and display higher signal strengths. Besides, tree ring cellulose $\delta^{18}O$ has significant correlations with climatic parameters, while ring width does not. Based on these findings, I found that tree ring cellulose $\delta^{18}O$ can provide a useful alternative approach to cross-date tree samples, especially for trees in tropical areas that cannot be cross-dated using ring width due to frequent endogenous disturbance or the lack of distinct limiting factors for tree growth. In future study, tree ring cellulose $\delta^{18}O$ should be used for cross-dating if either cross-dating by ring width does not perform well due to the absence of a dominant external limiting factor or frequent endogenous disturbance, or if the number of samples is limited (e.g., archeological samples).

3) Tree ring cellulose $\delta^{18}O$ show significant correlations with precipitation, temperature, PDSI and water level of Mekong River in the monsoon season during the period of 1951-2002. In addition, spatial correlation analysis reveals that tree ring cellulose $\delta^{18}O$ represents regional hydroclimate variations in central Indo-China.

4) The $\delta^{18}O$-based reconstruction of PDSI shows that the wetter periods were identified as AD 1660-1695, AD 1705-1790, whereas the drier periods mainly occurred during AD 1630–1660, AD 1900-1940 and AD 1954-2002 in the Southeast Asia. The comparison among four tree ring $\delta^{18}O$-based Asian summer monsoon proxies in Himalaya and Southeast Asia indicates that Asian summer monsoon intensity decreased during the last 200 years.

5) The spatial correlation analysis between tree ring cellulose $\delta^{18}O$ and global SST and the time series correlation analysis between tree-ring cellulose $\delta^{18}O$ and the MEI during the investigated period (1872-2002) reveal that tree ring cellulose $\delta^{18}O$ in northern Southeast Asia is a promising proxy for ENSO reconstruction. Combining ENSO-sensitive proxy in northern Laos and Vietnam, annual MEI and local ENSO events history are reconstructed during the period of 1605-2002, which is consistent with global ENSO events.

In future, more effort should be made to build up ENSO-sensitive tree-ring network in Southeast Asia and ENSO-sensitive proxy in Pacific. This could be foundation for understanding spatial teleconnection of ENSO variability in past and for climate modeling to generate more reliable forecasts of ENSO variations in future.

Acknowledgement

There are dozens of people that have largely contributed to my PhD study. I would like to express my deep gratitude for their kind support, suggestion, encouragement, etc.

First and foremost, I would like to acknowledge Prof. Takeshi Nakatsuka for accepting me as a PhD student in Nagoya University and making my PhD study possible. He taught me all the things on how to do experiments and handle the mass spectrometer, which are essential part for not only my PhD study but also for my future study. Due to his rich knowledge, I learned many things on isotopes from him. His diligence and serious attitude on sciences set an excellent example for me. Besides, he always support me to learn more (attending international conferences visiting other labs) and to realize my own idea (fieldwork in China). Thank you very much for your encouragement, support and guidance during the last three years.

I would like to thank Dr. Masaki Sano. He provided a lot of *Fokienia hodginsii* samples in Laos and Vietnam for my study. He also taught me about basic process of tree ring research, such as cross-dating by COEFCHA and ARSTAN software. In addition, he helped me on laboratory work and shared much useful information with me.

I would like to thank Dr. Qiang Li. He who is my tutor in my first semester helped me to start my life in Japan smoothly, and provided many helps on my study and life.

I am grateful to Prof. Osamu Abe, Dr. Maki Morimoto, Dr. Naoyuki Kurita, Ms. Zhen Li, Mr. Oishi of Nagoya University. They kindly help me on laboratory work or give me some good comments.

Finally, I express my deepest sense of gratitude to my wife, father, mother and parents in-law for their patience, love, and unyielding support.

Chenxi Xu
July, 2013
Nagoya University,
Nagoya, Japan

This work is a part of the Special Program of Sciences of Atmosphere and Hydrosphere for International Students in Nagoya University. Chenxi Xu is supported by the scholarship from the Japanese Ministry of Education, Culture, Sports, Science and Technology (MEXT).

References

Abram N, Gagan M, Cole J, Hantoro W, Mudelsee M (2008) Recent intensification of tropical climate variability in the Indian Ocean, Nature Geoscience 1:849-853.

Allison G, Gat J, Leaney F (1985) The relationship between deuterium and oxygen-18 delta values in leaf water, Chemical Geology: Isotope Geoscience section 58:145-156.

Anchukaitis, K., M. Evans, N. Wheelwright, and D. Schrag (2008) Stable isotope chronology and climate signal calibration in neotropical montane cloud forest trees. Journal of Geophysical Research 113, G03030, doi:10.1029/2007JG000613.

Anchukaitis, K., M. Evans (2010), Tropical cloud forest climate variability and the demise of the Monteverde golden toad, Proceedings of the National Academy of Sciences, 107(11), 5036-5040, doi:10.1073/pnas.0908572107

Anderson W, Bernasconi S, McKenzie J, Saurer M (1998) Oxygen and carbon isotopic record of climatic variability in tree ring cellulose (Picea abies): an example from central Switzerland (1913-1995), Journal of Geophysical Research 103:31625.

Araguas-Araguas L, Froehlich K, Rozanski K (1998) Stable isotope composition of precipitation over southeast Asia, Journal of Geophysical Research 103:28721.

Barbour M, Schurr U, Henry B, Wong S, Farquhar G (2000) Variation in the oxygen isotope ratio of phloem sap sucrose from castor bean. Evidence in support of the Péclet effect, Plant Physiology 123:671-680.

Barbour, M, J. S. Roden, G. D. Farquhar, and J. R. Ehleringer (2004) Expressing leaf water and cellulose oxygen isotope ratios as enrichment above source water reveals evidence of a Péclet effect, Oecologia, 138(3), 426-435, doi:10.1007/s00442-003-1449-3.

Berkelhammer M, Stott L (2012) Secular temperature trends for the southern Rocky Mountains over the last five centuries, Geophysical Research Letters 39:L17701.

Buckley, B., B. Cook, A. Bhattacharyya, D. Dukpa, and V. Chaudhary (2005), Global surface temperature signals in pine ring-width chronologies from southern monsoon

Asia, Geophysical Research Letters, 32, L20704, doi:10.1029/2005GL023745.

Buckley, B. M., O. Tongjit, R. Poonsrt, and N. Pumijumnong (2001) A dendrometer band study of Teak (Tectona grandis L.F.) in north Thailand, Palaeobotanist, 50, 83-87.

Buckley, B. M., K. Palakit, K. Duangsathaporn, P. Sanguantham, and P. Prasomsin (2007a) Decadal scale droughts over northwestern Thailand over the past 448 years: links to the tropical Pacific and Indian Ocean sectors, Climate dynamics, 29(1), 63-71, doi:10.1007/s00382-007-0225-1.

Buckley, B. M., K. Duangsathaporn, K. Palakit, S. Butler, V. Syhapanya, and N. Xaybouangeun (2007b) Analyses of growth rings of Pinus merkusii from Lao PDR, Forest Ecology and Management, 253(1-3), 120-127, doi:10.1016/j.foreco.2007.07.018.

Buckley, B. M., K. J. Anchukaitis, D. Penny, R. Fletcher, E. R. Cook, M. Sano, L. C. Nam, A. Wichienkeeo, T. T. Minh, and T. M. Hong (2010), Climate as a contributing factor in the demise of Angkor, Cambodia, Proceedings of the National Academy of Sciences, 107(15), 6748-6752, doi:10.1073/pnas.0910827107.

Braganza K, Gergis JL, Power SB, Risbey JS, Fowler AM (2009) A multiproxy index of the El Nino–Southern Oscillation, AD 1525–1982. J. Geophys. Res 114:D05106.

Brendel, O., P. P. M. Iannetta, and D. Stewart (2000), A rapid and simple method to isolate pure alpha-cellulose, Phytochemical Analysis, 11(1), 7-10.

Burk R, Stuiver M (1981) Oxygen isotope ratios in trees reflect mean annual temperature and humidity. Science 211:1417.

Cook, E. (1985), A time series analysis approach to tree ring standardization, The University of Arizona, Tucson, the United States.

Cook ER, Meko DM, Stahle DW, Cleaveland MK (1999) Drought reconstructions for the continental United States*. Journal of Climate 12:1145-1162.

Chen, T. C., and J. Yoon (2000), Interannual variation in Indochina summer monsoon rainfall: Possible mechanism, Journal of climate, 13(11), 1979-1986.

Cook E, Kevin J. Anchukaitis, Brendan M. Buckley, Rosanne D. D'Arrigo, Gordon C. Jacoby, Wright WE (2010) Asian Monsoon Failure and Megadrought During the Last Millennium. Science 328:486-489.

Chu G, Sun Q, Yang K, Li A, Yu X, Xu T, Yan F, Wang H, Liu M, Wang X (2011) Evidence for decreasing South Asian summer monsoon in the past 160 years from varved sediment in Lake Xinluhai, Tibetan Plateau. Journal of Geophysical Research 116:D02116.

Craig, H., and L. I. Gordon (1965), Deuterium and oxygen 18 variations in the ocean and the marine atmosphere, Stable Isotopesin Oceanography Studies and Paleotemperatures.Spoleto, July 26-27, Coniglio Nazionale delle Ricerche. Laboratorio di Geologia Nucleare, Pisa, pp. 1-222.

Cole JE, Dunbar RB, McClanahan TR, Muthiga NA (2000) Tropical Pacific forcing of decadal SST variability in the western Indian Ocean over the past two centuries. Science 287:617-619.

Conroy JL, Restrepo A, Overpeck JT, Steinitz-Kannan M, Cole JE, Bush MB, Colinvaux PA (2009) Unprecedented recent warming of surface temperatures in the eastern tropical Pacific Ocean. Nature Geoscience 2:46-50.

D'Arrigo, R., M. Barbetti, M. Watanasak, and B. M. Buckley (1997), Progress in dendroclimatic studies of mountain pine in Northern Thailand, IAWA Journal, 18(4), 433-444.

D'Arrigo R, Palmer J, Ummenhofer CC, Kyaw NN, Krusic P (2011) Three centuries of Myanmar monsoon climate variability inferred from teak tree rings. Geophysical Research Letters 38:L24705.

Dai, A., K. E. Trenberth, and T. Qian (2004), A global dataset of Palmer Drought Severity Index for 1870-2002: Relationship with soil moisture and effects of surface warming, Journal of Hydrometeorology, 5(6), 1117-1130.

Dansgaard, W. (1964), Stable isotopes in precipitation, Tellus, 16(4), 436-468.

da Silva RP, dos Santos J, Tribuzy ES, Chambers JQ, Nakamura S, Higuchi N (2002) Diameter increment and growth patterns for individual tree growing in Central Amazon, Brazil. Forest Ecology and Management 166:295-301.

Deniro, M., and S. Epstein (1979), Relationship between the oxygen isotope ratios of terrestrial plant cellulose, carbon dioxide, and water, Science, 204(4388), 51-53.

Diaz, H. F., and V. Markgraf (2000), El Nino and the Southern Oscillation: multiscale

variability and global and regional impacts, Cambridge University Press, New York.

Dongmann, G., H. Nuernberg, H, H. Foerstel, K. Wagener (1974), On the enrichment of $H_2{}^{18}O$ in the leaves of transpiring plants, Radiation and Environmental Biophysics, 11, 41–52.

English, N. B., D. L. Dettman, and D. G. Williams (2010), A 26-year stable isotope record of humidity and El Ni o-enhanced precipitation in the spines of saguaro cactus, Carnegiea gigantea, Palaeogeography, Palaeoclimatology, Palaeoecology, 293(1-2), 108-119.

Esper J, Frank D, Battipaglia G, Büntgen U, Holert C, Treydte K, Siegwolf R, Saurer M (2010) Low‐frequency noise in d13C and d18O tree ring data: A case study of Pinus uncinata in the Spanish Pyrenees. Global Biogeochem. Cycles 24.

Evans, M, and D. Schrag (2004), A stable isotope-based approach to tropical dendroclimatology, Geochimica et Cosmochimica Acta, 68, 3295–3305, doi:10.1016/j.gca.2004.01.006.

Evans M (2007) Toward forward modeling for paleoclimatic proxy signal calibration: A case study with oxygen isotopic composition of tropical woods. Geochemistry. Geophysics. Geosystems 8.

Fan F, Mann ME, Ammann CM (2009) Understanding Changes in the Asian Summer Monsoon over the Past Millennium: Insights from a Long-Term Coupled Model Simulation. Journal of Climate 22:1736-1748.

Flanagan, L. B., J. P. Comstock, and J. R. Ehleringer (1991), Comparison of modeled and observed environmental influences on the stable oxygen and hydrogen isotope composition of leaf water in Phaseolus vulgaris L, Plant Physiology, 96(2), 588.

Flanagan LB, Phillips SL, Ehleringer JR, Lloyd J, Farquhar GD (1994) Effect of changes in leaf water oxygen isotopic composition on discrimination against $C^{18}O^{16}O$ during photosynthetic gas exchange. Functional Plant Biology 21:221-234.

Fritts, H. C. (1976), Tree rings and climate, London, New York, San Francisco.: Academic Press.

Fu C, Z. Ma (2008), Global change and regional aridification (in Chinese). Chinese J Atmos Sci, 32(4), 752—760

Gagen, M., D. McCarroll, N. J. Loader, and I. Robertson (2011a), Stable Isotopes in Dendroclimatology: Moving Beyond 'Potential', Dendroclimatology, 147-172, DOI 10.1007/978-1-4020-5725-0_6.

Gagen, M., E. Zorita, D. McCarroll, G. H. F. Young, H. Grudd, R. Jalkanen, N. J. Loader, I. Robertson, and A. Kirchhefer (2011b), Cloud response to summer temperatures in Fennoscandia over the last thousand years, Geophysical Research Letters, 38, L05701, doi:10.1029/2010GL046216.

Gaudinski J, Dawson T, Quideau S, Schuur E, Roden J, Trumbore S, Sandquist D, Oh S, Wasylishen R (2005) Comparative analysis of cellulose preparation techniques for use with ^{13}C, ^{14}C, and ^{18}O isotopic measurements. Anal. Chem 77:7212-7224.

Gergis JL, Fowler AM (2009) A history of ENSO events since AD 1525: implications for future climate change. Climatic change 92:343-387.

Goswami, B. N., V. Krishnamurthy, and H. Annamalai (1999), A broadscale circulation index for the interannual variability of the Indian summer monsoon, Q. J. R. Meteorol. Soc., 125(554), 611 –633.

Green J (1963) Methods in carbohydrate chemistry. Whistler RL, Green JW.

Gill, A. E. (1980), Some simple solutions for heat-induced tropical circulation, Q. J. R. Meteorol. Soc., 106, 447– 462.

Grießinger J, Bräuning A, Helle G, Thomas A, Schleser G (2011) Late Holocene Asian summer monsoon variability reflected by $\delta^{18}O$ in tree-rings from Tibetan junipers. Geophysical Research Letters 38:L03701.

Hill, S., J. Waterhouse, E. Field, V. Switsur, and R. AP (1995), Rapid recycling of triose phosphates in oak stem tissue, Plant, Cell & Environment, 18(8), 931-936.

Holmes R (1983) Computer-assisted quality control in tree-ring dating and measurement. Tree-ring bulletin 43:69-78.

Komonjinda, S. (2003), An analysis of rainfall, temperature and relative humidity in north Thailand: Application to paleoclimatology, MA thesis, Fac. of Environ. and Resour. Stud., Mahidol Univ., Salaya, Thailand.

Kumar KK, Rajagopalan B, Cane MA (1999) On the weakening relationship between the Indian monsoon and ENSO. Science 284:2156-2159.

Lau K, Yang S (1997) Climatology and interannual variability of the Southeast Asian summer monsoon. Advances in Atmospheric Sciences 14:141-162.

Leavitt S, Long A, Dean J (1985) Tree-ring dating through pattern-matching of stable-carbon isotope time series. Tree-ring 45:1.

Leavitt, S. (2010), Tree-ring C-H-O isotope variability and sampling, Science of The Total Environment, 408, 5244-5253, doi:10.1016/j.scitotenv.2010.07.057.

Li, J., S. P. Xie, E. R. Cook, G. Huang, R. D'Arrigo, F. Liu, J. Ma, and X. T. Zheng (2011a), Interdecadal modulation of El Nino amplitude during the past millennium, Nature Climate Change, 1(2), 114-118, doi:10.1038/nclimate1086.

Li Q (2011) Hydroclimate Variability in Semiarid North China from 1675 to 2003 Inferred from Oxygen Isotope Ratios of Tree Rings, Nagoya University, Nagoya.

Li, Q., T. Nakatsuka, K. Kawamura, Y. Liu, and H. Song (2011b), Regional hydroclimate and precipitation δ18O revealed in tree-ring cellulose $\delta^{18}O$ from different tree species in semi-arid Northern China., Chemical Geology, 282, 19-28, doi:10.1016/j.chemgeo.2011.01.004.

Li, Z. H., N. Labbé, S. G. Driese, and H. D. Grissino-Mayer (2011c), Micro-scale analysis of tree-ring δ18O and δ13C on α-cellulose spline reveals high-resolution intra-annual climate variability and tropical cyclone activity, Chemical Geology, 284,138-147, doi:10.1016/j.chemgeo.2011.02.015.

Libby LM, Pandolfi LJ, Payton PH, Marshall J, Becker B, Giertz-Sienbenlist V (1976) Isotopic tree thermometers, Nature, 261, pp. 284–290

Loader N, Robertson I, Barker A, Switsur V, Waterhouse J (1997) An improved technique for the batch processing of small wholewood samples to α-cellulose. Chemical Geology 136:313-317.

Loader N., P. Santillo, J. Woodman-Ralph, J. Rolfe, M. Hall, M. Gagen, I. Robertson, R. Wilson, C. Froyd, D. McCarroll (2008), Multiple stable isotopes from oak trees in southwestern Scotland and the potential for stable isotope dendroclimatology in maritime climatic regions, Chemical Geology, 252, 62-71, doi:10.1016/j.chemgeo.2008.01.006

Kahmen A, Sachse D, Arndt SK, Tu KP, Farrington H, Vitousek PM, Dawson TE (2011)

Cellulose $\delta^{18}O$ is an index of leaf-to-air vapor pressure difference (VPD) in tropical plants. Proceedings of the National Academy of Sciences 108:1981.

Kripalani R, Oh J, Kulkarni A, Sabade S, Chaudhari H (2007) South Asian summer monsoon precipitation variability: Coupled climate model simulations and projections under IPCC AR4. Theoretical and Applied Climatology 90: 133-159.

Managave, S., M. Sheshshayee, A. Bhattacharyya, and R. Ramesh (2010), Intra-annual variations of teak cellulose δ18O in Kerala, India: implications to the reconstruction of past summer and winter monsoon rains, Climate dynamics, 1-13, doi:10.1007/s00382-010-0917-9.

Managave, S., M. Sheshshayee, R. Ramesh, H. Borgaonkar, S. Shah, and A. Bhattacharyya (2011), Response of cellulose oxygen isotope values of teak trees in differing monsoon environments to monsoon rainfall, Dendrochronologia,25, 89-97. doi:10.1016/j.dendro.2010.05.00

Mann ME, Bradley RS, Hughes MK (2000) Long-term variability in the El Nino Southern Oscillation and associated teleconnections. Cambridge University Press, Cambridge, UK.

Mann ME, Lees JM (1996) Robust estimation of background noise and signal detection in climatic time series. Climatic change 33:409-445.

McCarroll D, Loader N (2004) Stable isotopes in tree rings. Quaternary Science Reviews 23:771-801.

McGregor S, Timmermann A, Timm O (2010) A unified proxy for ENSO and PDO variability since 1650. Climate of the Past 6:1-17.

Meehl G, Arblaster J (2003) Mechanisms for projected future changes in south Asian monsoon precipitation. Climate dynamics 21:659-675.

Meehl GA, Hu A (2006) Megadroughts in the Indian monsoon region and southwest North America and a mechanism for associated multidecadal Pacific sea surface temperature anomalies. J Climate 19:1605–1623.

Nakatsuka T (2007) Reconstruction of paleo-climate using tree-ring oxygen isotopic ratios. Low Temp. Sci. 65:49–56.

Ohashi Y, Sahri MH, Yoshizawa N, Itoh T (2005) Annual rhythm of xylem growth in

rubberwood (Hevea brasiliensis) trees grown in Malaysia. Holzforschung 55:151-154.

Ortlieb L (2000) Multiscale Variability and Global and Regional Impacts, chap. The documented historical record of El Nino events in Peru: An update of the Quinn Record (Sixteenth through Nineteenth Centuries). Cambridge University Press, pp. 207–295.

Overpeck JT, Cole JE (2007) Climate change: Lessons from a distant monsoon. Nature 445:270-271.

Palmer, W. C. (1965), Meteorological drought. Research Paper No. 45. U.S. Dept. of Commerce Weather Bureau, Washington.

Poussart, P., and D. Schrag (2005), Seasonally resolved stable isotope chronologies from northern Thailand deciduous trees, Earth and Planetary Science Letters, 235(3-4), 752-765, doi:10.1016/j.epsl.2005.05.012

Poussart, P., M. Evans, and D. Schrag (2004), Resolving seasonality in tropical trees: multi-decade, high-resolution oxygen and carbon isotope records from Indonesia and Thailand, Earth and Planetary Science Letters, 218(3-4), 301-316, doi:10.1016/S0012-821X(03)00638-1.

Pumijumnong N, Eckstein D (2011) Reconstruction of pre-monsoon weather conditions in northwestern Thailand from the tree-ring widths of Pinus merkusii and Pinus kesiya. Trees:1-8.

Quinn WH (1993) The Large-scale ENSO event, the El Nino, and other important features. Bull. Inst. fr. études andines 22:13-34.

Raffalli-Delerce, G., V. Masson-Delmotte, J. Dupouey, M. Stievenard, N. Breda, and J. Moisselin (2004), Reconstruction of summer droughts using tree-ring cellulose isotopes: a calibration study with living oaks from Brittany (western France), Tellus B, 56(2), 160-174, doi: 10.1111/j.1600-0889.2004.00086.x.

Robertson I, Waterhouse J, Barker A, Carter A, Switsur V (2001) Oxygen isotope ratios of oak in east England: implications for reconstructing the isotopic composition of precipitation. Earth and Planetary Science Letters 191:21-31.

Risi C, Bony S, Vimeux F, Descroix L, Ibrahim B, Lebreton E, Mamadou I, Sultan B (2008) What controls the isotopic composition of the African monsoon precipitation? Insights from event‐based precipitation collected during the 2006 AMMA field campaign.

Geophysical Research Letters 35.

Roden J (2008) Cross-dating of tree ring $\delta^{18}O$ and $\delta^{13}C$ time series. Chemical Geology 252:72-79.

Roden JS, Lin G, Ehleringer JR (2000) A mechanistic model for interpretation of hydrogen and oxygen isotope ratios in tree-ring cellulose. Geochimica et Cosmochimica Acta 64:21-35.

Rozendaal DM, Zuidema PA (2011) Dendroecology in the tropics: a review. Trees 25:3-16.

Sano M, Buckley B, Sweda T (2009) Tree-ring based hydroclimate reconstruction over northern Vietnam from Fokienia hodginsii: eighteenth century mega-drought and tropical Pacific influence. Climate dynamics 33:331-340.

Sano M, Ramesh R, Sheshshayee M, Sukumar R (2011) Increasing aridity over the past 223 years in the Nepal Himalaya inferred from a tree-ring $\delta^{18}O$ chronology. The Holocene.

Sano M, Xu C, Nakatsuka T (2012) A 300-year Vietnam hydroclimate and ENSO variability record reconstructed from tree ring $\delta^{18}O$. Journal of Geophysical Research 117:D12115.

Shi, C., V. Masson-Delmotte, C. Risi, T. Eglin, M. Stievenard, M. Pierre, X. Wang, J. Gao, F. M. Breon, and Q. B. Zhang (2011), Sampling strategy and climatic implications of tree-ring stable isotopes on the southeast Tibetan Plateau, Earth and Planetary Science Letters, doi:10.1016/j.epsl.2010.11.014.

Singhrattna N, Rajagopalan B, Kumar KK, Clark M (2005) Interannual and interdecadal variability of Thailand summer monsoon season. Journal of Climate 18:1697-1708.

Singhrattna, N., M. Babel, and S. Perret (2009), Hydroclimate variability and its statistical links to the large-scale climate indices for the Upper Chao Phraya River Basin, Thailand, Hydrology and Earth System Sciences Discussions, 6, 6659-6690, doi: 10.1175/JCLI3364.1.

Smith TM, Reynolds RW, Peterson TC, Lawrimore J (2008) Improvements to NOAA's historical merged land-ocean surface temperature analysis (1880-2006). Journal of Climate 21:2283-2296.

Spiecker, H., K. Mielik inen, M. K hl, and J. Skovsgaard (1996), Growth Trends in

European Forests, 372 pp., Springer Berlin.

Sternberg, L. (2009), Oxygen stable isotope ratios of tree-ring cellulose: the next phase of understanding, New Phytologist, 181(3), 553-562, doi: 10.1111/j.1469-8137.2008.02661.x.

Sternberg, L. D. S. L., M. J. Deniro, and R. A. Savidge (1986), Oxygen isotope exchange between metabolites and water during biochemical reactions leading to cellulose synthesis, Plant Physiology, 82(2), 423.

Sternberg L, Ellsworth PFV (2011) Divergent Biochemical Fractionation, Not Convergent Temperature, Explains Cellulose Oxygen Isotope Enrichment across Latitudes. PloS one 6:e28040.

Tan M (2013) Circulation effect: response of precipitation $\delta^{18}O$ to the ENSO cycle in monsoon regions of China. Climatic Dynamics, DOI 10.1007/s00382-013-1732-x

Thompson LG, Mosley-Thompson E, Davis ME, Mashiotta TA, Henderson KA, Lin P-N, Tandong Y (2006) Ice core evidence for asynchronous glaciation on the Tibetan Plateau. Quaternary International 154:3-10.

Treydte KS, Schleser GH, Helle G, Frank DC, Winiger M, Haug GH, Esper J (2006) The twentieth century was the wettest period in northern Pakistan over the past millennium. Nature 440:1179-1182.

Ueda H, Iwai A, Kuwako K, Hori ME (2006) Impact of anthropogenic forcing on the Asian summer monsoon as simulated by eight GCMs. Geophysical Research Letters 33:L06703.

Van Oldenborgh, G. J., and G. Burgers (2005) Searching for decadal variations in ENSO precipitation teleconnections, Geophysical Research Letters, 32(15), L15701, doi:10.1029/2005GL023110.

Vecchi GA, Clement A, Soden BJ (2008) Examining the tropical Pacific's response to global warming. Eos, Transactions American Geophysical Union 89:81.

Vuille, M., R. S. Bradley, M. Werner, R. Healy, and F. Keimig (2003) Modeling $\delta^{18}O$ in precipitation over the tropical Americas: 1. Interannual variability and climatic controls, Journal of Geophysical Research, 108(D6), 4174,

Vuille M, Werner M, Bradley R, Keimig F (2005) Stable isotopes in precipitation in the

Asian monsoon region. Journal of Geophysical Research 110:D23108.

Wang B, Clemens SC, Liu P (2003) Contrasting the Indian and East Asian monsoons: implications on geologic timescales. Marine Geology 201:5-21.

Wang B, LinHo (2002) Rainy Season of the Asian-Pacific Summer Monsoon. Journal of Climate 15:386-398.

Wang B, Wu R, Fu X (2000) Pacific-east Asian teleconnection: How does ENSO affect east Asian climate? Journal of Climate 13:1517-1536.

Wang, Y. J., H. Cheng, R. L. Edwards, Z. S. An, J. Y. Wu, C.-C. Shen, and J. A. Dorale (2001), A high-resolution absolute-dated late Pleistocene monsoon record from Hulu cave, China, Science, 294, 2345– 2348.

Webster PJ, Magaña VO, Palmer TN, Shukla J, Tomas RA (1998) Monsoons: Processes, predictability, and the prospects for prediction. Journal of Geophysical Research 103:14451-14510.

Webster PJ, Yang S (1992) Monsoon and ENSO: Selectively interactive systems. Quarterly Journal of the Royal Meteorological Society 118:877-926.

White, J. W. C., E. R. Cook, J. R. Lawrence, and S. Wallace (1985), The ratios of sap in trees: Implications for water sources and tree ring ratios, Geochimica et Cosmochimica Acta, 49(1), 237-246.

Wigley T, Briffa K, Jones P (1984) On the average value of correlated time series, with applications in dendroclimatology and hydrometeorology. Journal of Climate and Applied Meteorology 23:201-213.

Wilson A, Grinsted M (1977) $^{12}C/^{13}C$ in cellulose and lignin as palaeothermometers. Nature 265:133-135.

Wilson R, Cook E, D'Arrigo R, Riedwyl N, Evans MN, Tudhope A, Allan R (2010) Reconstructing ENSO: the influence of method, proxy data, climate forcing and teleconnections. Journal of Quaternary Science 25:62-78.

Wilson R, Tudhope A, Brohan P, Briffa K, Osborn T, Tett S (2006) Two-hundred-fifty years of reconstructed and modeled tropical temperatures. Journal of Geophysical Research 111:C10007.

Wolter, K., and M. S. Timlin (2011), El Nino/Southern Oscillation behaviour since 1871 as

diagnosed in an extended multivariate ENSO index (MEI. ext), International Journal of Climatology, 31, 1074-1087, doi: 10.1002/joc.2336.

Xu C, Sano M, Nakatsuka T (2011) Tree ring cellulose $\delta^{18}O$ of Fokienia hodginsii in northern Laos: A promising proxy to reconstruct ENSO? Journal of Geophysical Research 116:D24109.

Xu H, Hong Y, Hong B (2012) Decreasing Asian summer monsoon intensity after 1860 AD in the global warming epoch. Climate dynamics:1-10.

Yakir, D., and M. J. DeNiro (1990), Oxygen and hydrogen isotope fractionation during cellulose metabolism in Lemna gibba L, Plant Physiology, 93(1), 325.

Yancheva G, Nowaczyk NR, Mingram J, Dulski P, Schettler G, Negendank JFW, Liu J, Sigman DM, Peterson LC, Haug GH (2007) Influence of the intertropical convergence zone on the East Asian monsoon. Nature 445:74-77.

Young GHF, Demmler JC, Gunnarson BE, Kirchhefer AJ, Loader NJ, McCarroll D (2011) Age trends in tree ring growth and isotopic archives: A case study of Pinus sylvestris L. from northwestern Norway. Global Biogeochemical Cycles 25:GB2020.

Zhang P, Cheng H, Edwards RL, Chen F, Wang Y, Yang X, Liu J, Tan M, Wang X (2008) A test of climate, sun, and culture relationships from an 1810-year Chinese cave record. Science 322:940.

Zhu M, Stott L, Buckley B, Yoshimura K (2012) 20th century seasonal moisture balance in Southeast Asian montane forests from tree cellulose $\delta^{18}O$. Climatic change:1-13.